Application Note

Bluetooth® Angle of Arrival (AoA) Antenna Design

ABSTRACT

This application note helps hardware and RF designers implement a compact PCB antenna array to accurately measure the angle of arrival (AoA) of an incoming Bluetooth® signal. Antenna design considerations are discussed along with antenna array test results and methods for calculating the AoA.

Table of Contents

List of Figures

List of Tables

Trademarks

Bluetooth® is a registered trademark of Bluetooth SIG, Inc.
Skyworks® is a registered trademark of Skyworks Solutions, Inc..
3M® is a registered trademark of 3M.
All trademarks are the property of their respective owners.

1 Introduction

Bluetooth® angle of arrival (AoA) measures the angle or direction a Bluetooth Low Energy (BLE) transmitted signal approaches a Bluetooth receiver. To calculate the AoA, two or more antennas are required to measure the phase of an incoming signal.

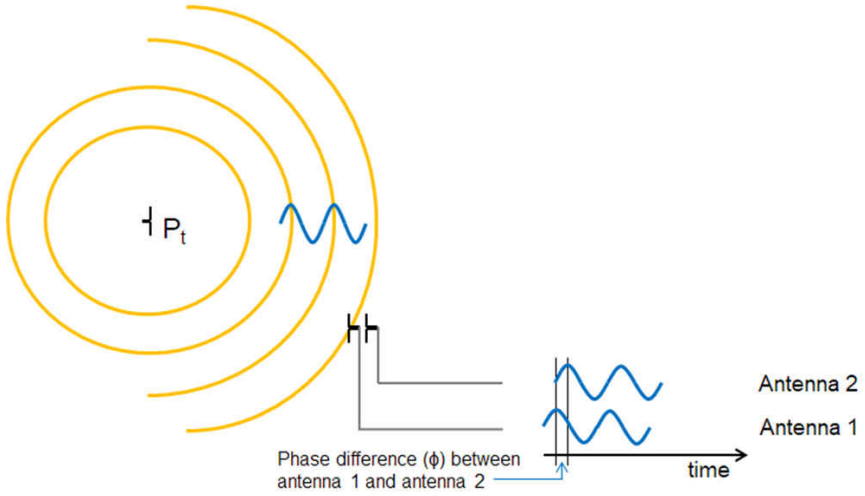

Figure 1-1. Transmitter Phase Measured by Antenna Array

The phase measurements from each antenna are used to calculate the AoA and determine the direction of the transmitted signal. This application note explains AoA antenna design considerations, shows test results from some antenna arrays, and demonstrates how to calculate the AoA measurement from the phase measurement data of the antenna array. For more background information on Bluetooth AoA, see the *Bluetooth Low Energy Angle of Arrival (AoA) SimpleLink Academy* and the *BLE-Stack User's Guide*.

2 Angle of Arrival Antenna Design Considerations

To calculate the AoA, the incoming RF carrier phase must be measured with minimal impact to the signal phase of the carrier itself using two or more co-located antennas. Therefore, there are several considerations to understand when designing a Bluetooth Low Energy antenna array. First, to determine which antenna is closest to the transmitted signal, the antenna phase centers must be within ½ λ of each other, discussed in Section 2.1. Consequently, antenna spacing becomes a concern as undesired coupling can occur reducing the efficiency of the antenna array. Furthermore, to avoid additional phase measurement errors and any added calibration requirements, the phase centers of the antenna should be constant. If the phase center shifts due to the direction of the incoming signal, the phase center change must be accounted for in the AoA calculation. Finally, with any antenna design, other antenna basics such as grounding and efficiency should be understood to improve the overall effectiveness of the receiver and ensure minimal interference from reflections. Another aspect of the AoA hardware design is the RF switch required to switch between two or more antennas. It is important to understand the RF switching times to calculate the AoA measurement and meet the Bluetooth 5.1 specification as well as understand the RF switch specifications to ensure good performance while optimizing cost.

2.1 Antenna Spacing

The two receiving antenna phase centers must be within ½ λ (maximum phase difference of 180°) to easily determine which antenna is closer to the transmitter. In a two-antenna system, each antenna takes turns measuring phase. Once phase measurements are completed, the phase difference between the antennas is used to calculate the AoA. If the difference is greater than 180°, the true phase difference could be incorrectly interpreted. Figure 2-1 shows an example of a Bluetooth Low Energy transmitting node 180° from an antenna array with ¾ λ distance between antenna phase centers.

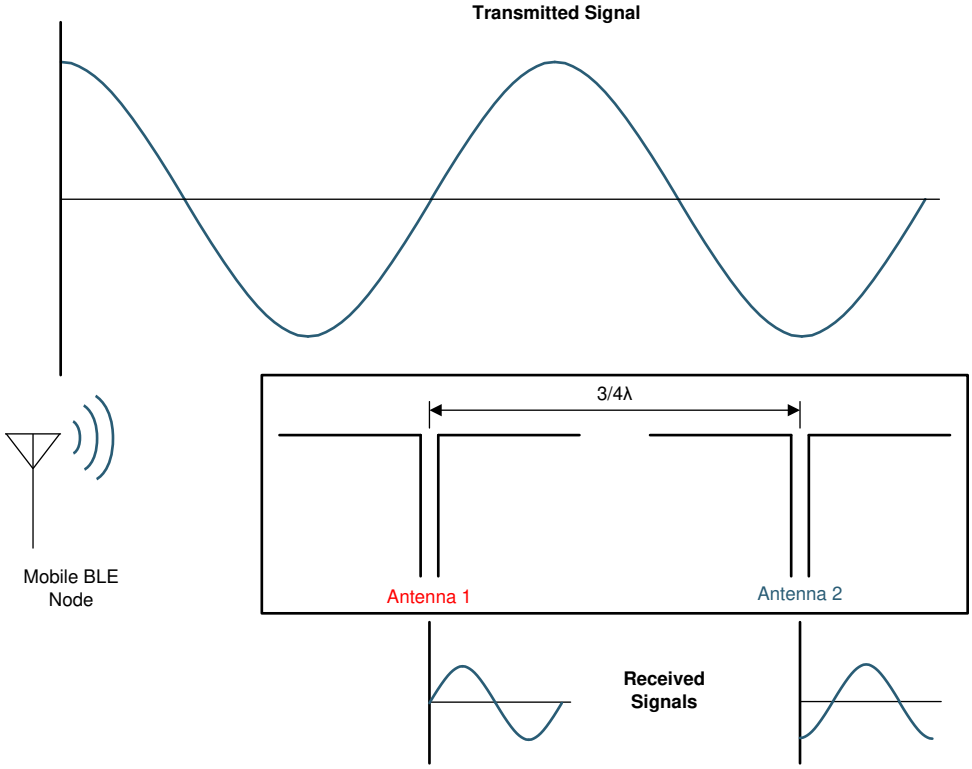

Figure 2-1. Antenna Array With ¾ λ Spacing

Antenna 1 measures 0° and antenna 2 measures 270° (–90°), the phase difference should be calculated as 270°. However, the phase difference could be interpreted incorrectly as a 90° difference from 270° to 0° as the phase diagram in Figure 2-2 shows.

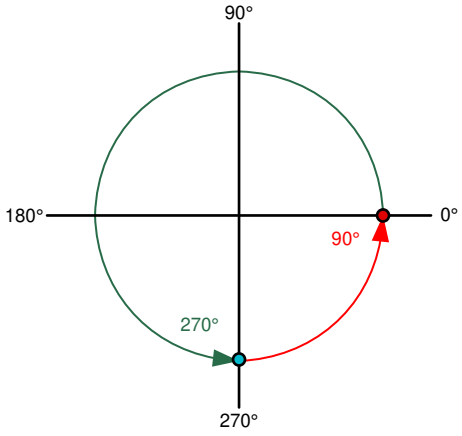

Figure 2-2. Example Phasor Diagram of ¾ λ Antenna Spacing

By ensuring the antennas are at max ½ λ, the phase difference range always falls from 0° to 180° (or –180°) and there is no issue determining which antenna is closer to the transmitting node because the lowest phase difference is always correct whether positive or negative as Figure 2-3 shows.

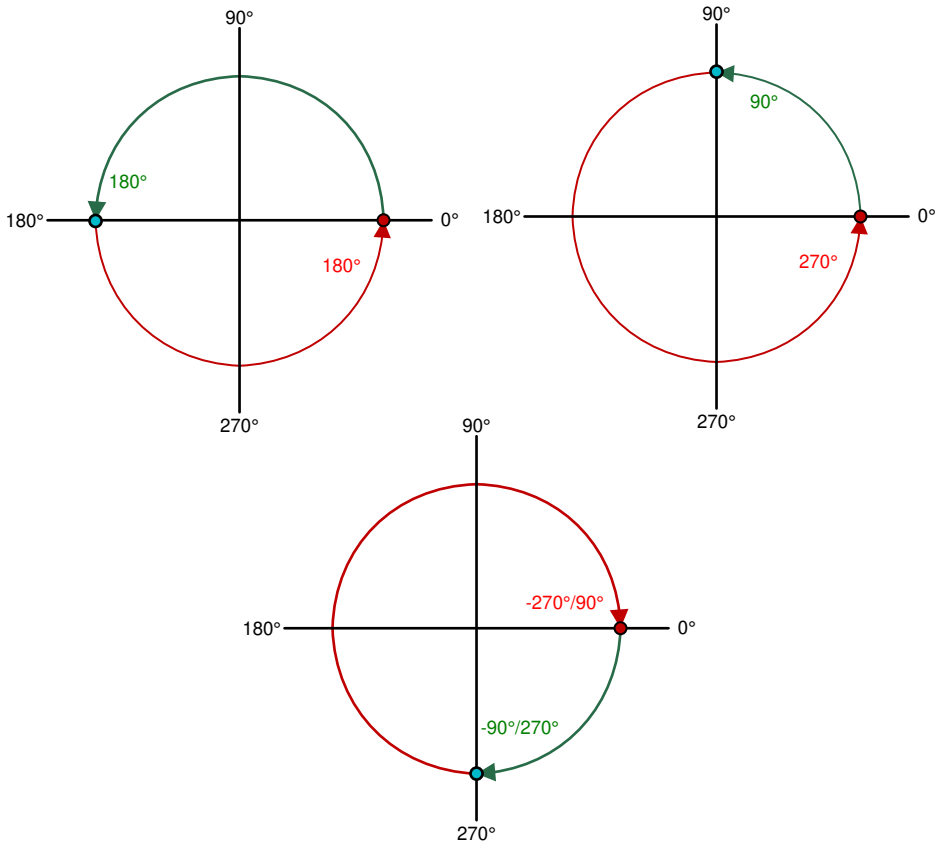

Figure 2-3. Phasor Diagram with ≤ ½ λ Antenna Spacing

If the antenna array is designed at the center of the Bluetooth spectrum (2.44 GHz), the antenna spacing must be less than or equal to 61.5 mm. Therefore, antenna coupling can become an issue affecting the antenna arrays efficiency.

2.2 RF Switch Considerations

RF switch characteristics that matter the most in an AoA application are the switching time, channel isolation, and number of channels. Switching time is important because the Bluetooth 5.1 specification requires 2-µs switch slots with the option of supporting quicker 1-µs switch slots.

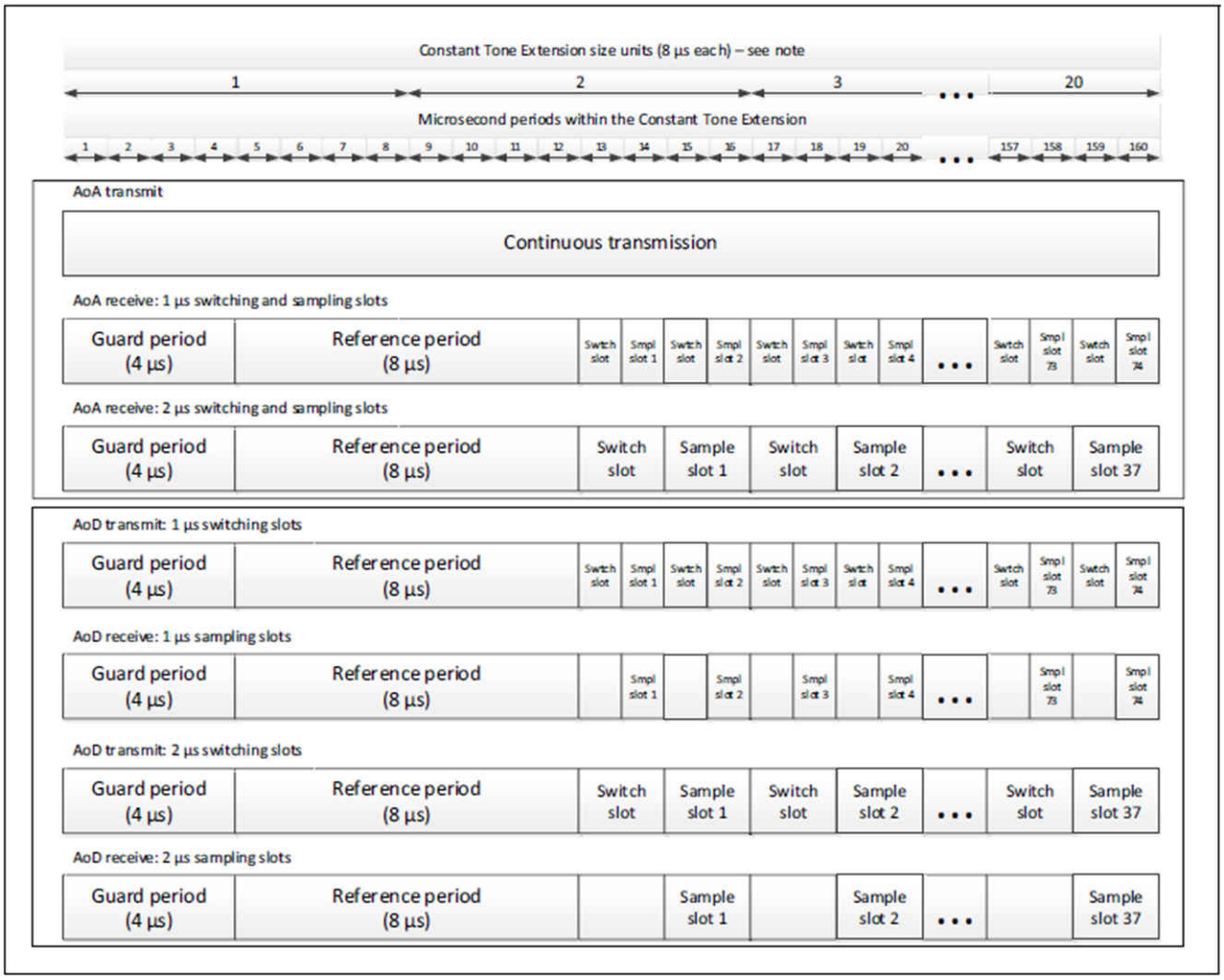

Figure 2-4. Constant Tone Extension Structure Bluetooth Specification v5.1

Therefore, the RF switch must be able to switch and settle within the specified switch slot time (whether 2 µs or 1 µs). It is important to note that IQ sampling begins 0.125 µs into a 1-µs slot and 1.125 µs into a 2-µs slot and ends 0.875 µs into a 1-µs slot and 1.875 µs into a 2-µs slot.

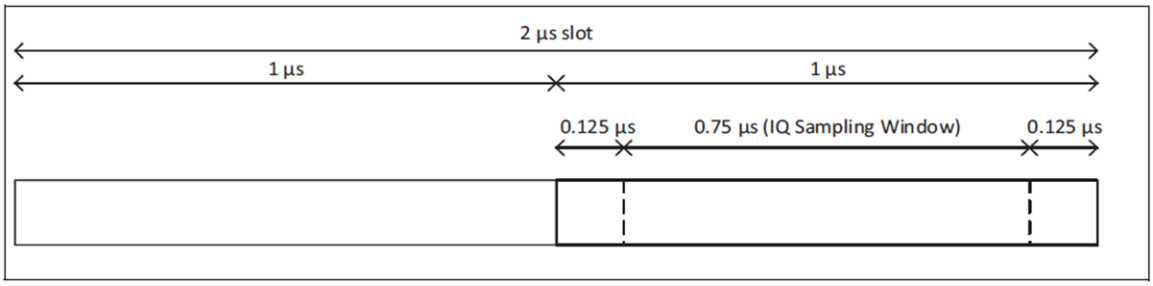

Figure 2-5. IQ Sampling Window for 2-µs Sample Slots

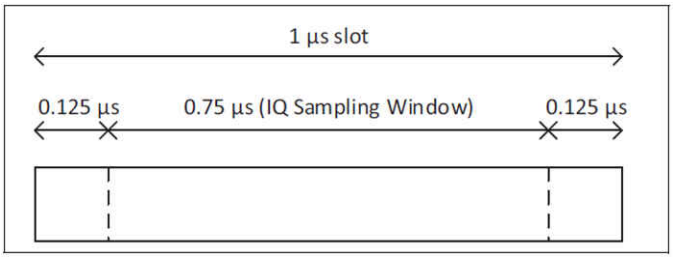

Figure 2-6. IQ Sampling Window for 1-µs Sample Slots

Channel isolation is also an important specification because it directly affects the efficiency of the system. The better the isolation between the RF channels, the better the overall efficiency of the RF system. Lastly, the number of channels is important as it plays a large factor in switch cost. Table 2-1 shows several viable RF switches, most of which have been implemented on TI angle of arrival printed circuit boards (PCB).

Table 2-1. Viable RF Switches for Bluetooth Low Energy AoA

Part Name	Manufacturer	Switch Type	Frequency Range (GHz)	Max 50% Control to 90/10% RF (ns)	Typical Isolation (dB)	Typical Insertion Loss (dB)	Automotive Qualification
SKY13408-465LF	Skyworks® Solutions, Inc.	SP3T	1–6	150	28	0.8	N/A
SKY13323-378LF	Skyworks Solutions, Inc.	SPDT	0.1–3	100	27	0.35	N/A
SKYA21001	Skyworks Solutions, Inc.	SPDT	0.2–3	250	23	0.4	AEC-Q100
RFSW8006QTR7	Qorvo	SP3T	0.1–4	500	25–31	0.6	AEC-Q100

3 Dipole Antenna Array

In this section, the dipole antenna array is discussed with focuses on the strengths and weaknesses of dipole antennas for AoA applications, the PCB implementation of the TIDA-01632 two dipole antenna array, and test results from the antenna array. The TIDA-01632 reference designs antenna array is based off the SimpleLink AoA Boosterpack dipole antennas which includes two arrays of three dipole antennas.

3.1 Dipole Antenna Strengths and Weaknesses

The dipole antenna has two big strengths and one weakness in an AoA application. The first strength is that dipole antennas have a constant phase center that is always at the feeding point (in the middle of the antenna). This is important as the antenna does not add any phase errors due to a shifting phase center. Second, the dipole antenna does not receive or transmit RF power in the direction of its own axis. Antenna coupling is therefore minimized even with the antennas being close to one another (phase centers <½ λ). Figure 3-1 shows the dipole antenna radiation pattern and phase center.

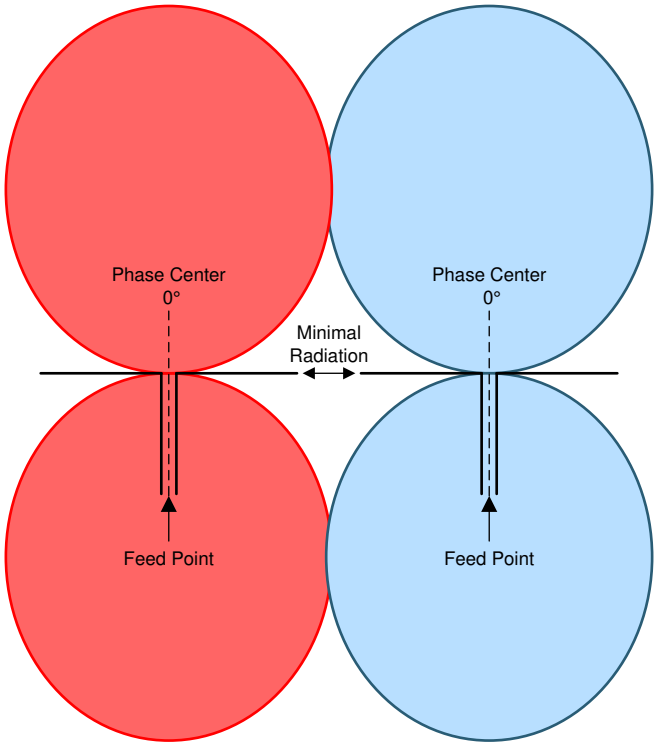

Figure 3-1. Dipole Antenna Radiation Pattern and Phase Center

The main weakness of the dipole antenna is that it is differential and requires isolation from ground. This requirement directly conflicts with the ground plane of the Bluetooth Low Energy receiver. If the ground plane is too close to the antenna, the antenna is effectively shorted because the ground plane reflects the inverse of the incoming wave. However, if the ground plane is further away, it will still reflect RF power back to the antenna and reduce its efficiency.

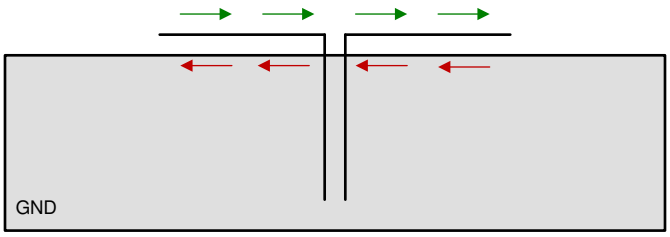

Figure 3-2. Boundary Current With GND Plane

To resolve the ground plane issue, a corrugated ground plane is implemented. The corrugated ground plane removes the boundary current by shifting the reflected phase 180° per finger by taking the boundary current on a ½ λ detour. Therefore, each segment cancels the effect of the neighboring segments and the net effect is zero current and an in-phase reflection as Figure 3-3 shows.

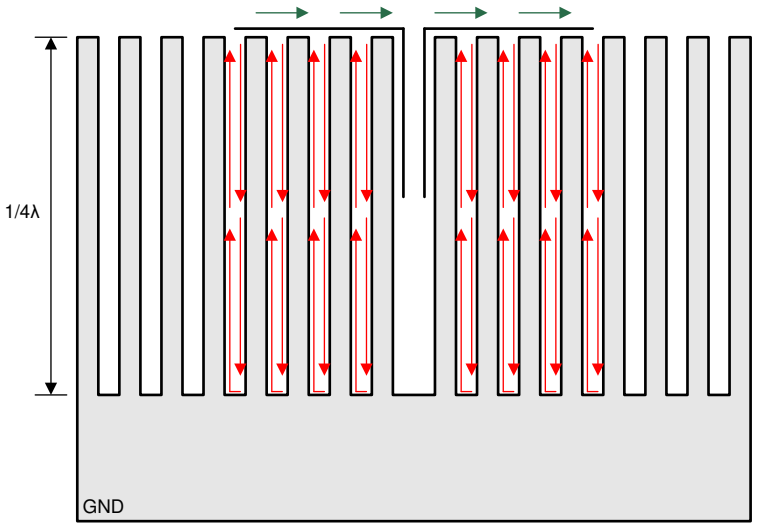

Figure 3-3. Boundary Current With Corrugated GND Plane

3.2 Angle Measurement Plane

A single dipole antenna array can measure the AoA of an incoming signal in one plane (that is, x, y, or z). If it is required to measure the direction of a signal in another plane, an additional dipole antenna array is required aligned parallel to the plane.

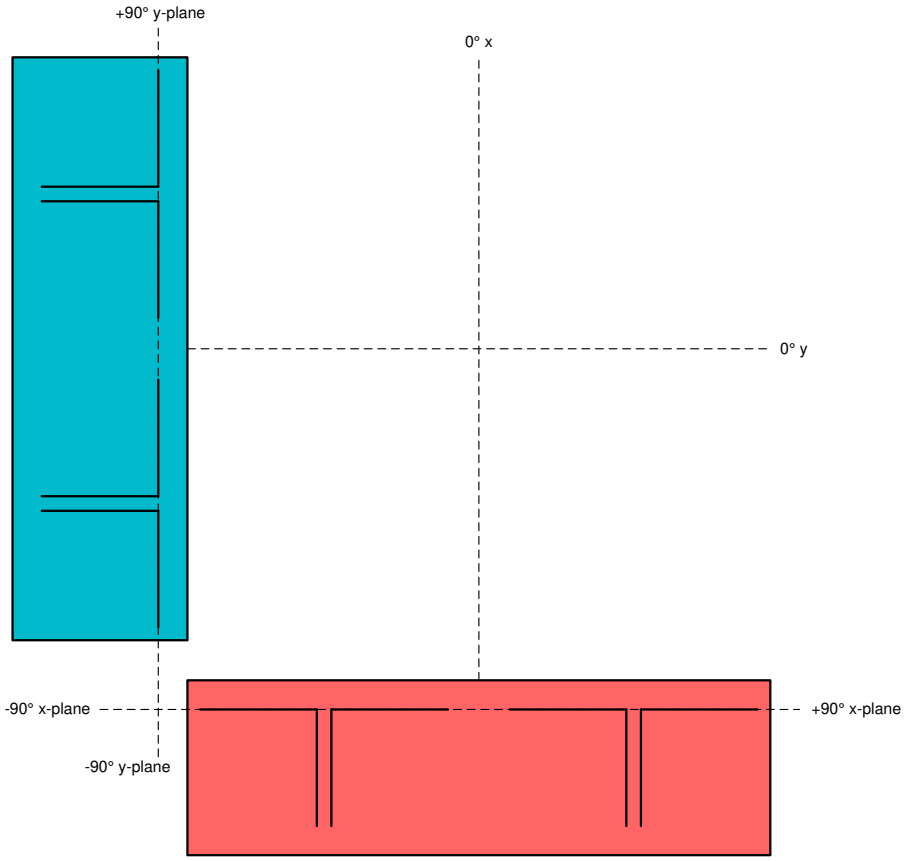

Figure 3-4. Antenna Array Orientation

This can be done on a single PCB such as the *SimpleLink™ Angle of Arrival BoosterPack* or by using another single antenna array PCB such as the *TIDA-01632* reference design in another orientation.

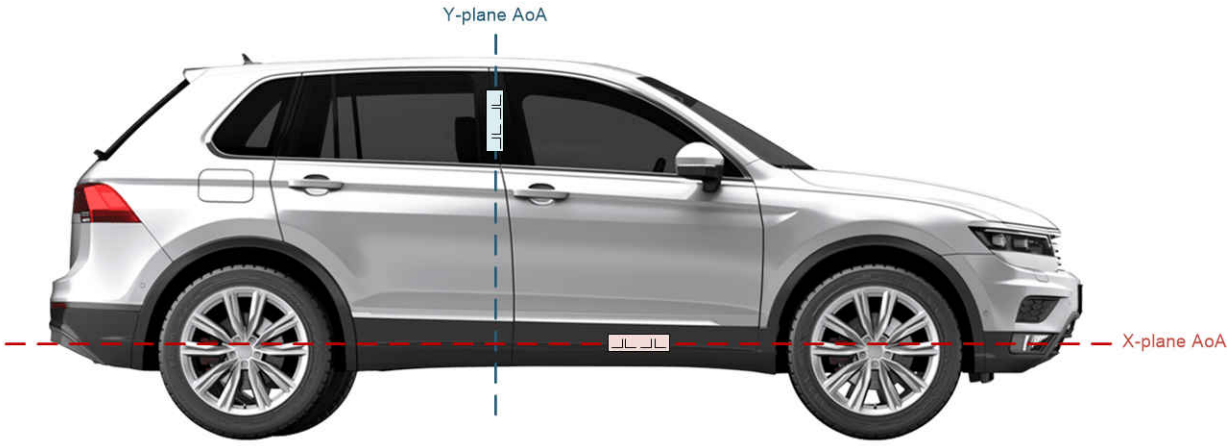

Figure 3-5. Measuring AoA in Two Planes With Multiple Dipole Antenna Arrays

In this example, the blue antenna array measures AoA in the y-plane, determining how high or low the key is located relative to the antenna array regardless of the key being located to the left, right, or center of the vehicle. The red antenna array measures AoA in the x-plane, determining if the key is to the left, right, or center of the vehicle passenger door regardless of how high or low the key is relative to the vehicle.

3.3 PCB Implementation

The ¼ λ dipole antennas were designed at the center of the Bluetooth Low Energy frequency spectrum (2.44 GHz) and therefore, have a length of about 30.8 mm. Notice that the phase centers are spaced 35 mm apart meeting the needed < ½ λ spacing requirement.

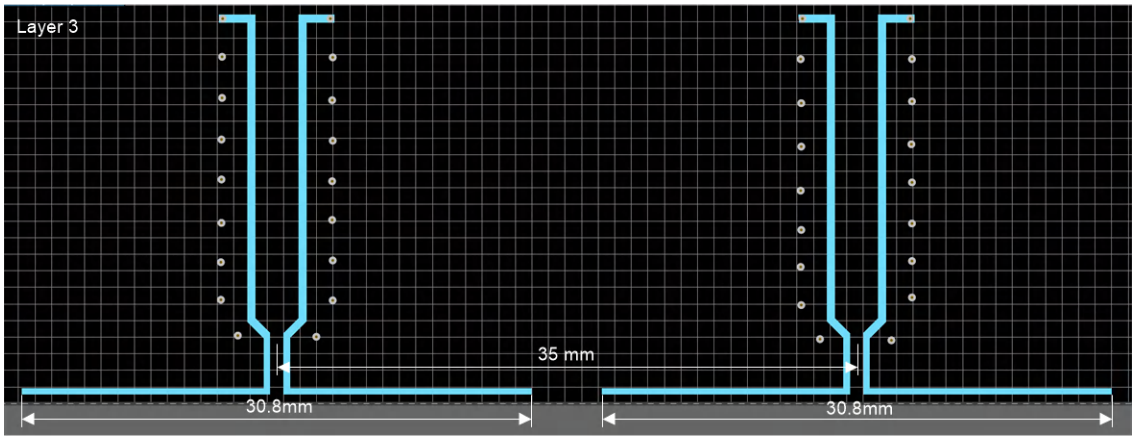

Figure 3-6. Layer 3 Dipole Spacing and Width

To transform the balanced (differential) signal to an unbalanced (single-ended) signal, a PCB Marchand balun was implemented on the layer below the dipole antenna (layer 4).

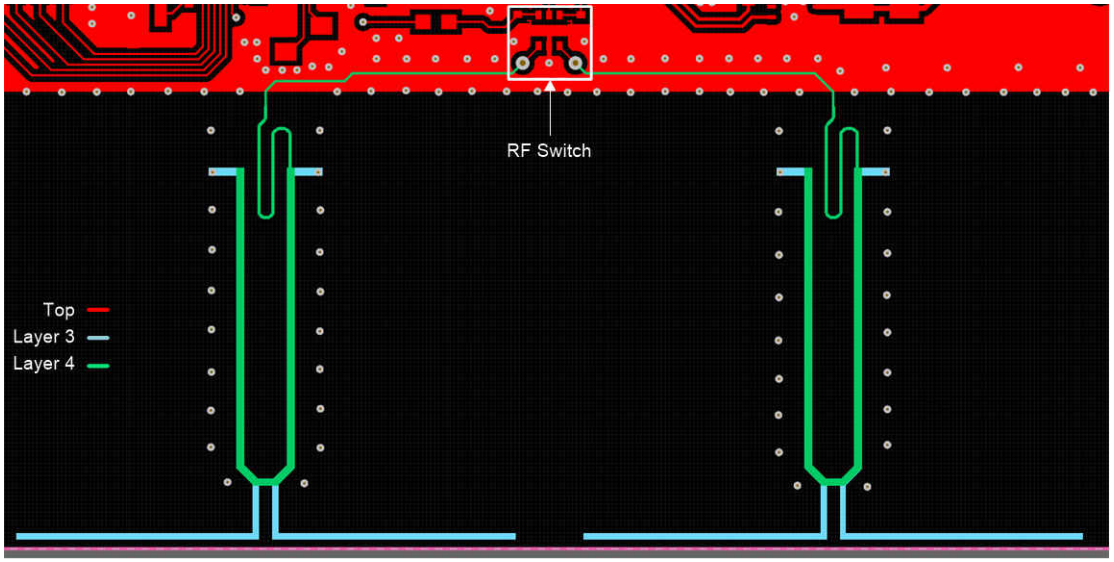

Figure 3-7. Layer 4 Marchand Balun

The Marchand balun was designed, simulated, and tested to ensure proper performance. The top section of the balun routed to the RF switch is used to match the 50-Ω impedance transmission line. Additionally, the board stack-up ensures proper spacing between the 3rd layer (dipole antenna) and the 4th layer (Marchand balun) for the correct amount of capacitive coupling between the two layers. Because the single-ended trace from the RF switch requires ground, the Marchand balun and dipole antenna feed traces are sandwiched between two identical ground planes, one on the 2nd layer and one on the 5th layer, as Figure 3-8 shows.

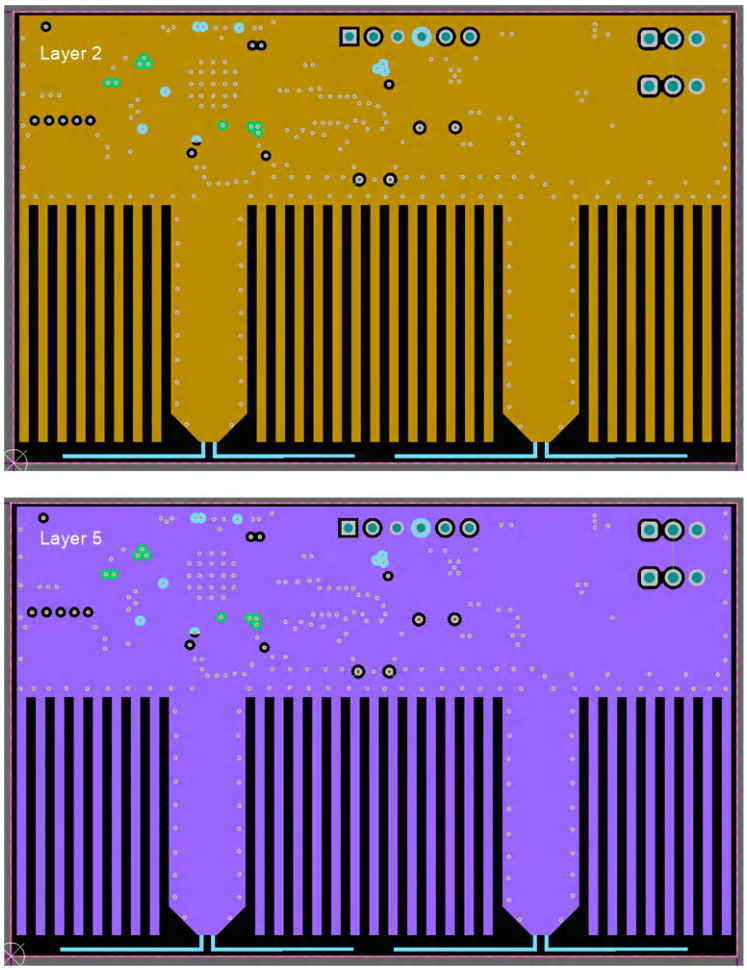

Figure 3-8. Layer 2 and 5 Ground Planes

Figure 3-9 through Figure 3-12 show the dimensions for the dipole antennas, Marchand balun, and GND planes.

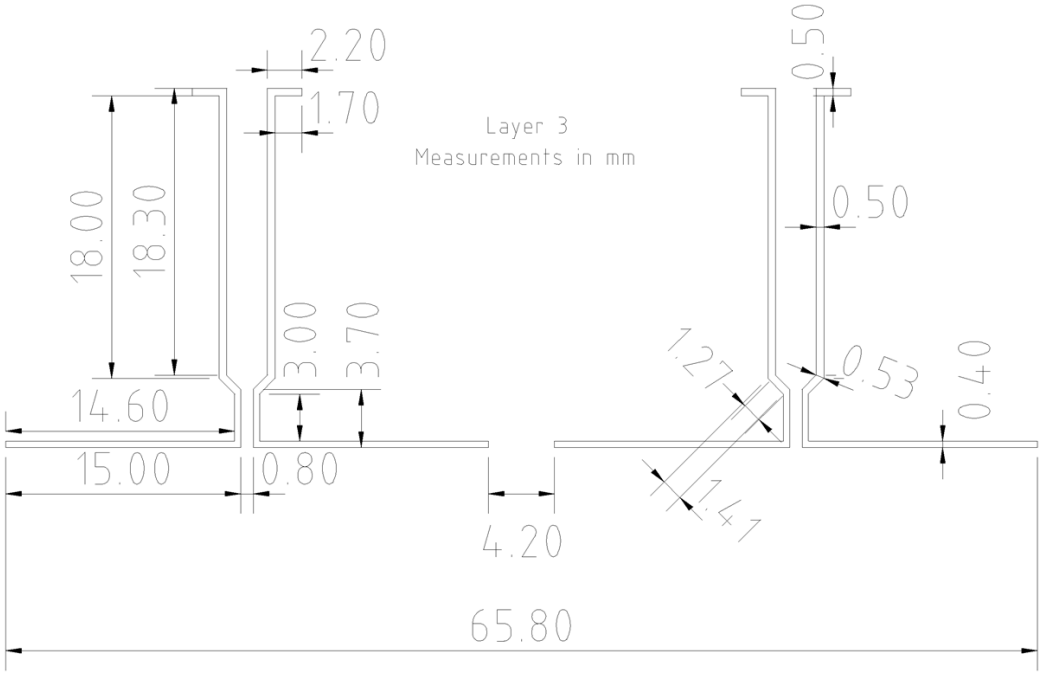

Figure 3-9. Layer 3 Dipole Antenna Dimensions

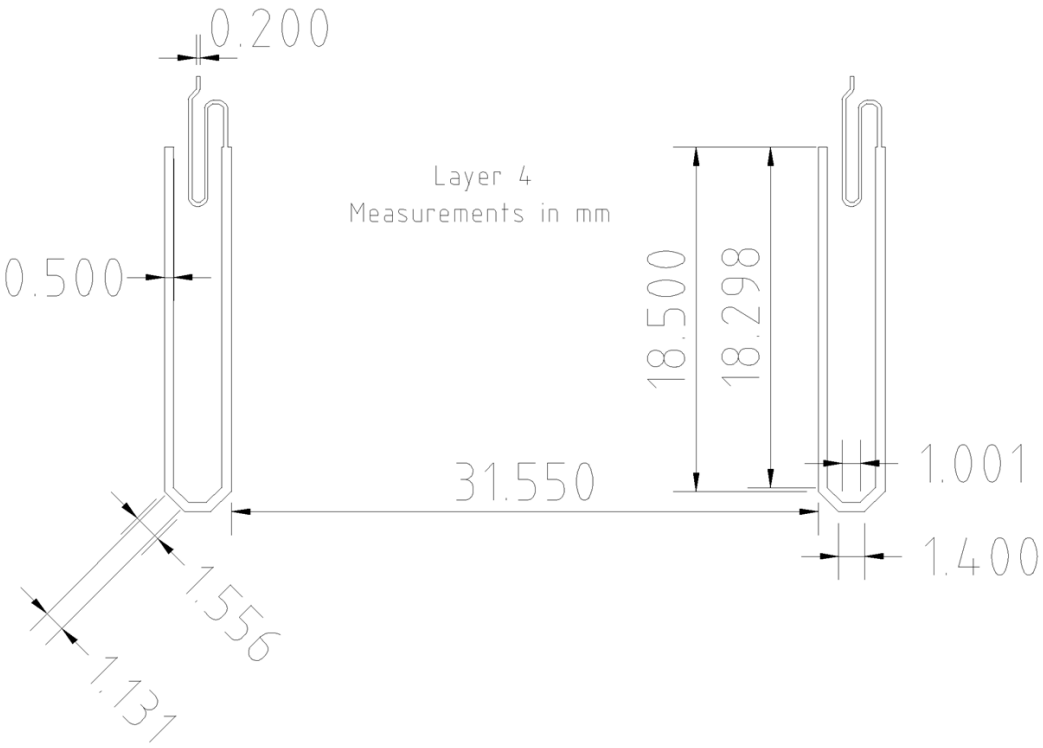

Figure 3-10. Layer 4 Marchand Balun Dimensions

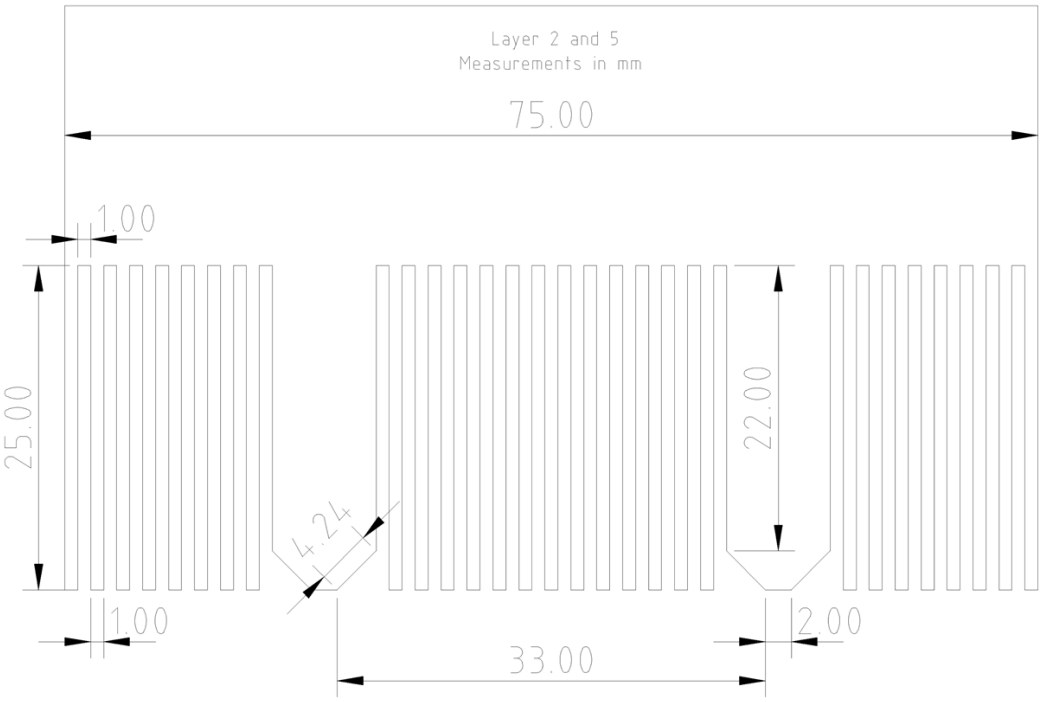

Figure 3-11. Layer 2 and 4 Ground Plane Dimensions

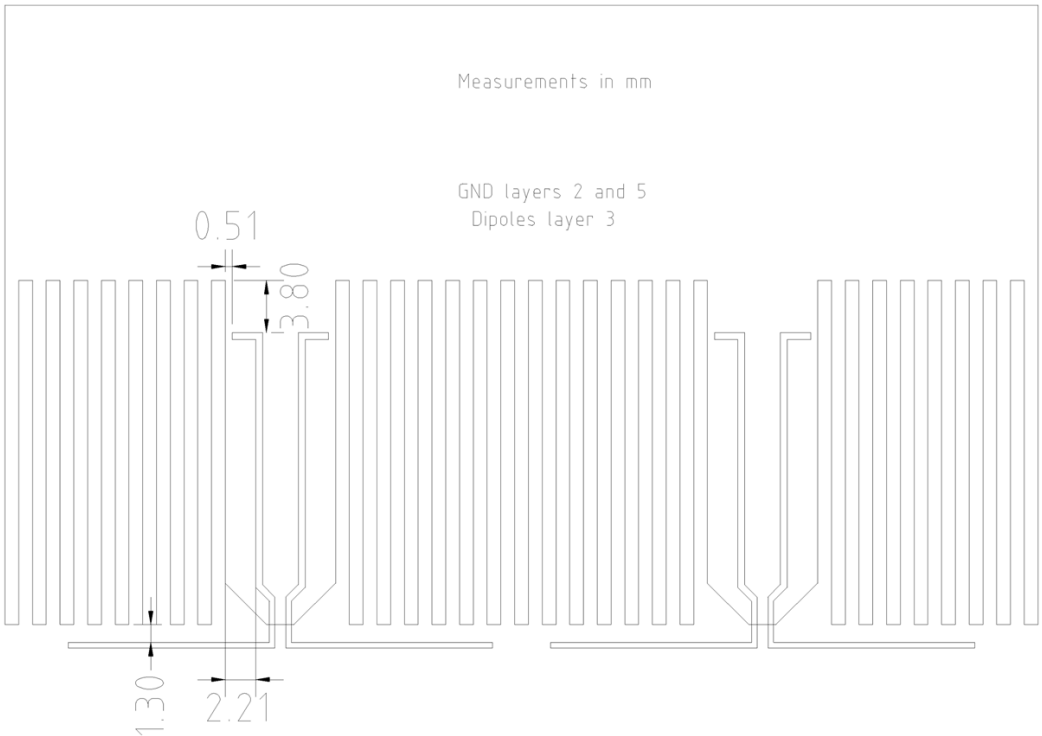

Figure 3-12. Dipole With Ground Plane Dimensions

Table 3-1. PCB Stack-up

Layer Name	Type	Material	Thickness (mm)	Dielectric Material	Dielectric Constant
Top Solder	Solder Mask/Coverlay	Surface Material	0.01016	Solder Resist	3.5
Top Layer	Signal	Copper	0.035		
Dielectric 1	Dielectric	Core	0.1	FR-4	4.1
Layer 2	Signal	Copper	0.01801		
Dielectric 2	Dielectric	Prepreg	0.2	FR-4	4.1
Layer 3	Signal	Copper	0.01901		
Dielectric 3	Dielectric	Core	0.1	FR-4	4.1
Layer 4	Signal	Copper	0.01801		
Dielectric 4	Dielectric	Prepreg	0.2	FR-4	4.1
Layer 5	Signal	Copper	0.01801		
Dielectric 5	Dielectric	Core	0.1	FR-4	4.1
Bottom Layer	Signal	Copper	0.035		
Bottom Solder	Solder Mask/Coverlay	Surface Material	0.01016	Solder Resist	3.5

See the TIDA-01632 Automotive Bluetooth® Low Energy car access satellite node reference design for more information on the design and for access to Gerber files, schematics, and more.

3.4 Two Dipole Array Test Results

The following sections show various test results based off the TIDA-01632 antenna design. All test results were taken in an anechoic chamber using the turntable shown in Figure 3-13, capable of rotating the base and the arm by 1° increments.

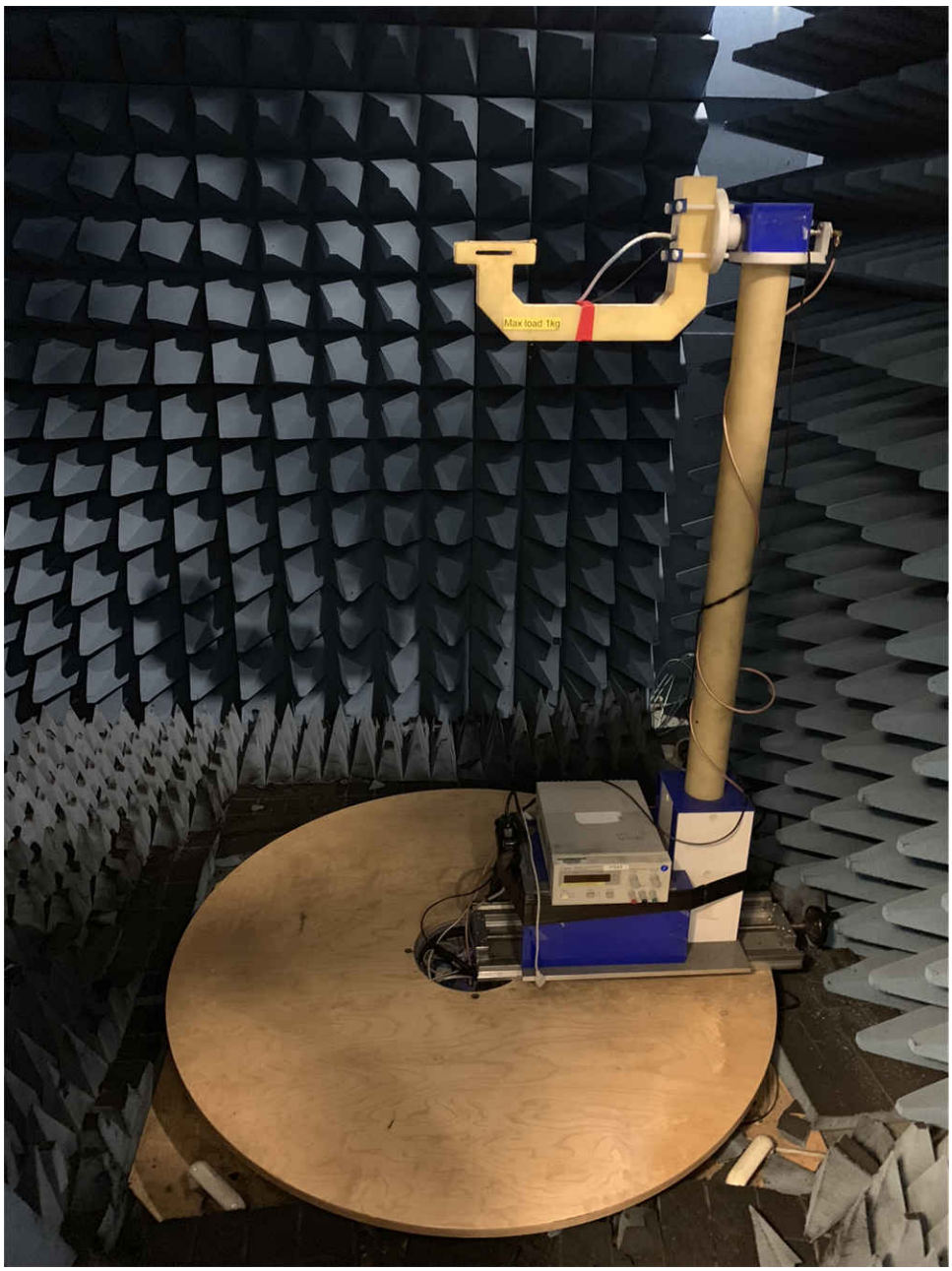

Figure 3-13. Turntable Test Setup

Figure 3-14 shows the TIDA-01632 PCB mounted on the arm of the turntable and Figure 3-15 shows the rest of the anechoic chamber.

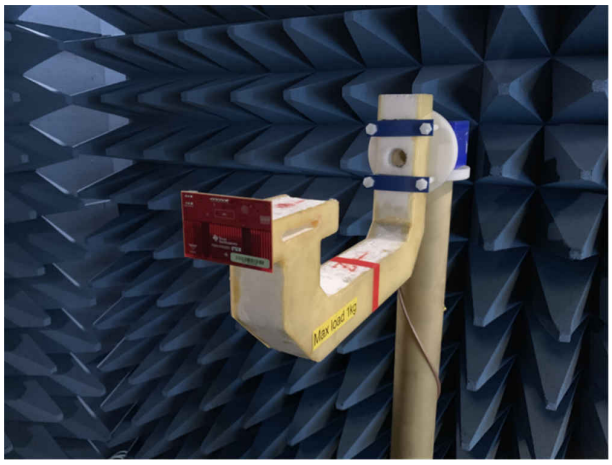

Figure 3-14. PCB Mounted on Turntable Arm

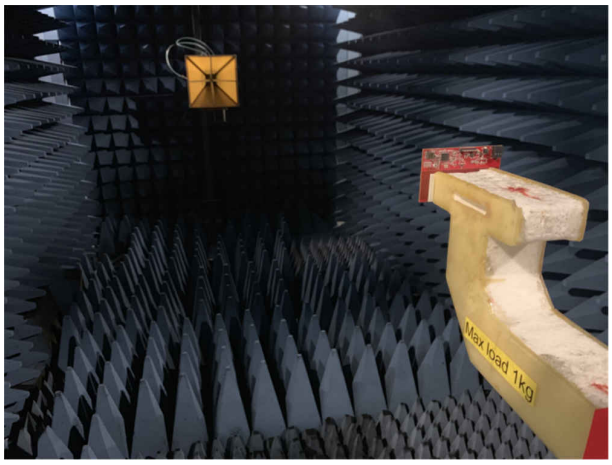

Figure 3-15. Anechoic Chamber

3.4.1 Total Radiated Power (TRP)

All radiation measurements are done on a TIDA-01632 PCB without any absorbing material or copper foil attached. The CC2640R2F-Q1 device on the TIDA-01632 is configured to output a constant wave at 2440 MHz with 0 dBm. The measured total radiated power (TRP) is –8.71 dBm and –8.97 dBm giving an antenna efficiency of around 14% (0.3 dB loss in the RF switch - SKYA21001). In the following measurements, the z-axis is perpendicular to the PCB, with the x-axis as the height and the y-axis as the length shown in Figure 3-16.

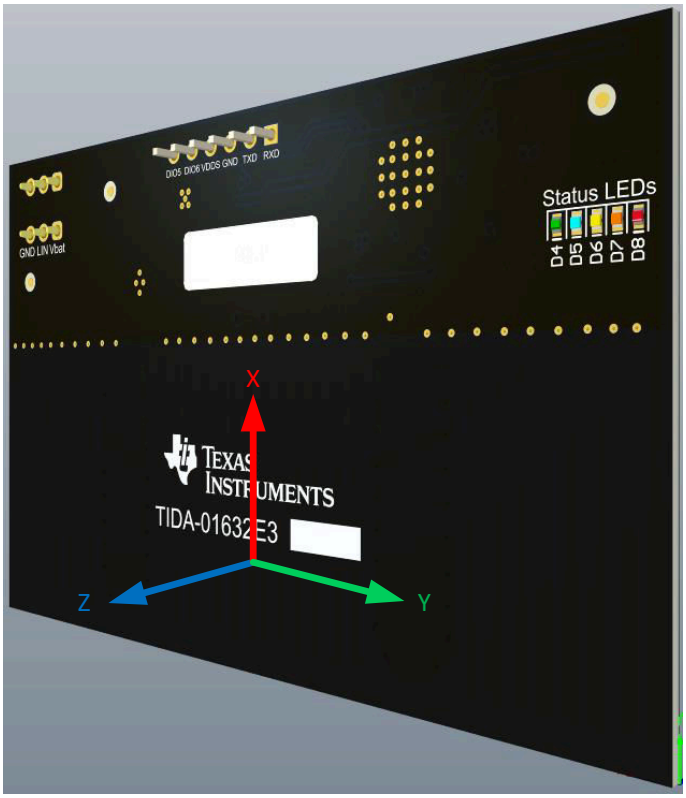

Figure 3-16. PCB Orientation for TRP Results

In the total radiated power plots, Theta represents the rotation of the PCB from the z-axis to the y-axis (turntable base rotating) and Phi represents the z-axis to the x-axis (rotating the arm from Figure 3-14).

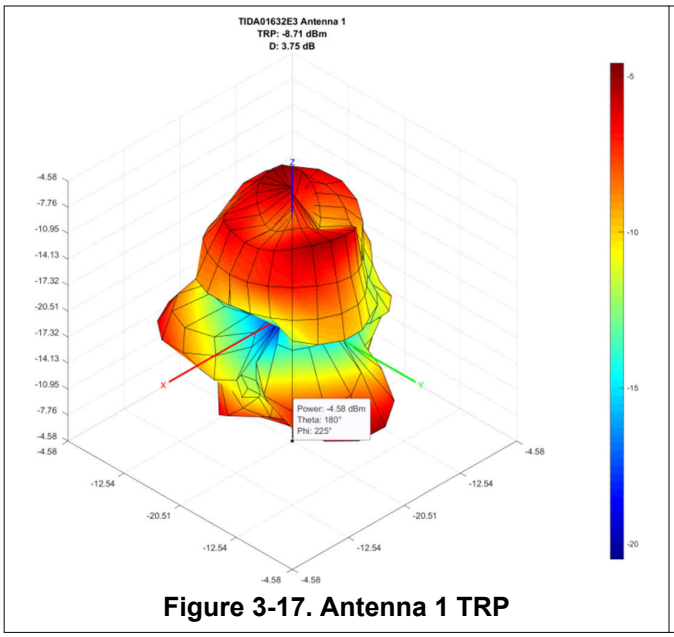

Figure 3-17. Antenna 1 TRP

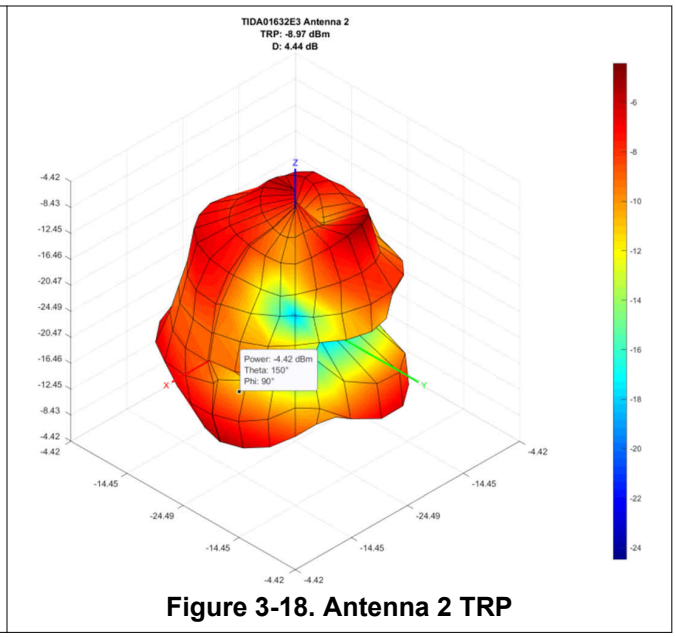

Figure 3-18. Antenna 2 TRP

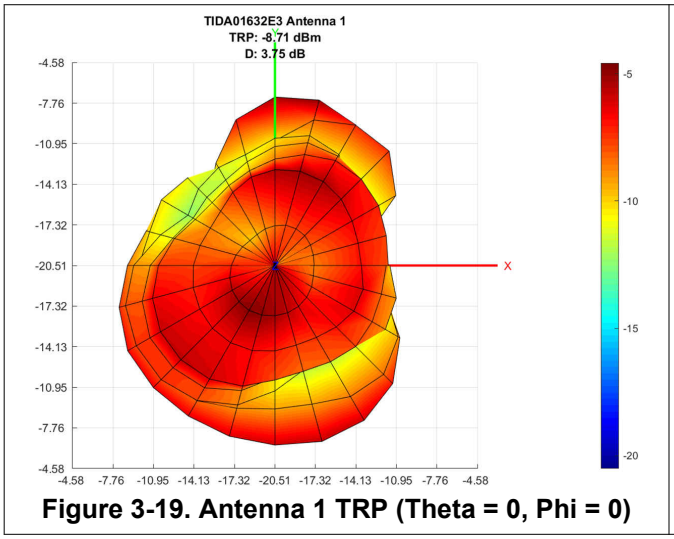

Figure 3-19. Antenna 1 TRP (Theta = 0, Phi = 0)

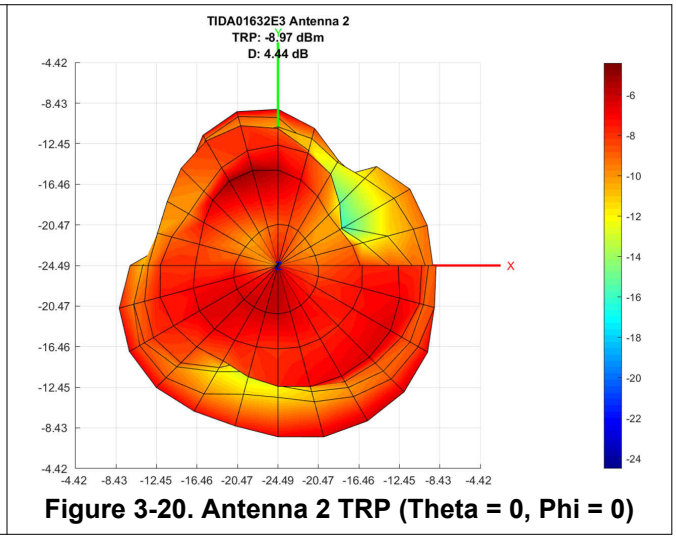

Figure 3-20. Antenna 2 TRP (Theta = 0, Phi = 0)

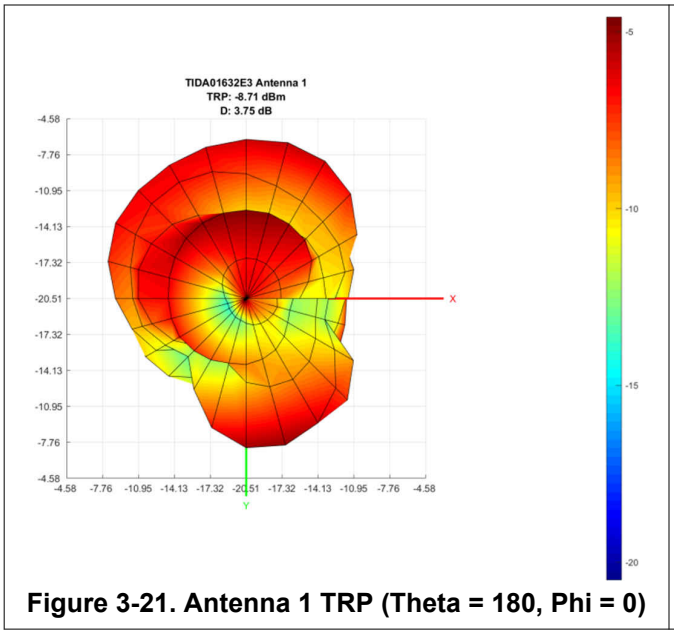

Figure 3-21. Antenna 1 TRP (Theta = 180, Phi = 0)

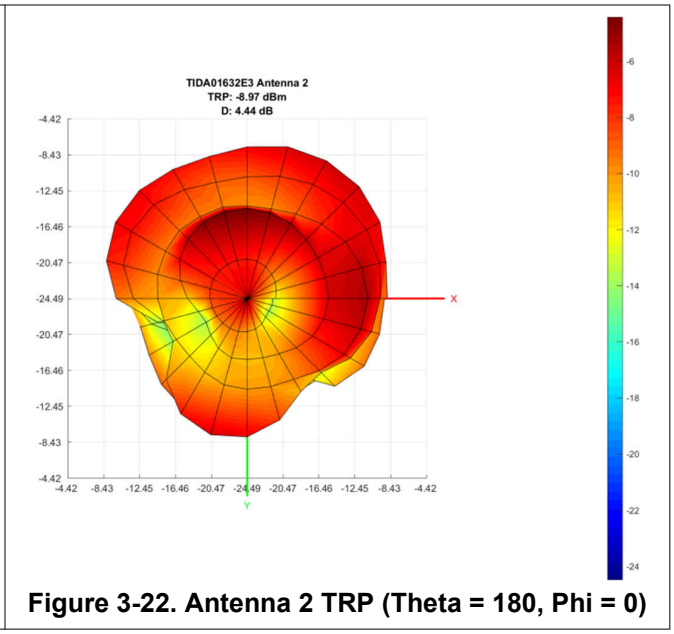

Figure 3-22. Antenna 2 TRP (Theta = 180, Phi = 0)

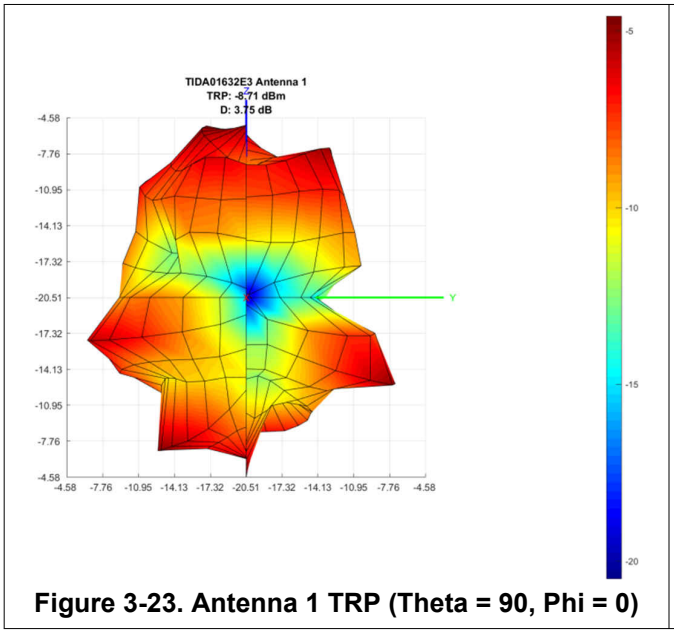

Figure 3-23. Antenna 1 TRP (Theta = 90, Phi = 0)

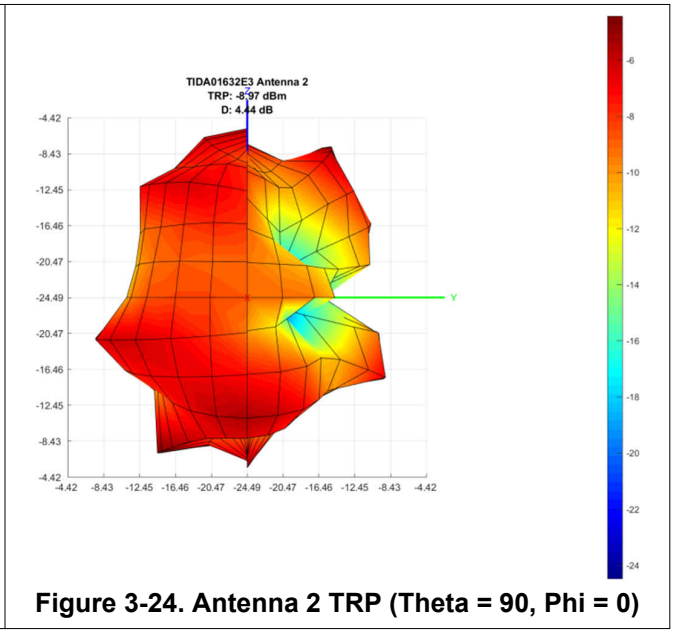

Figure 3-24. Antenna 2 TRP (Theta = 90, Phi = 0)

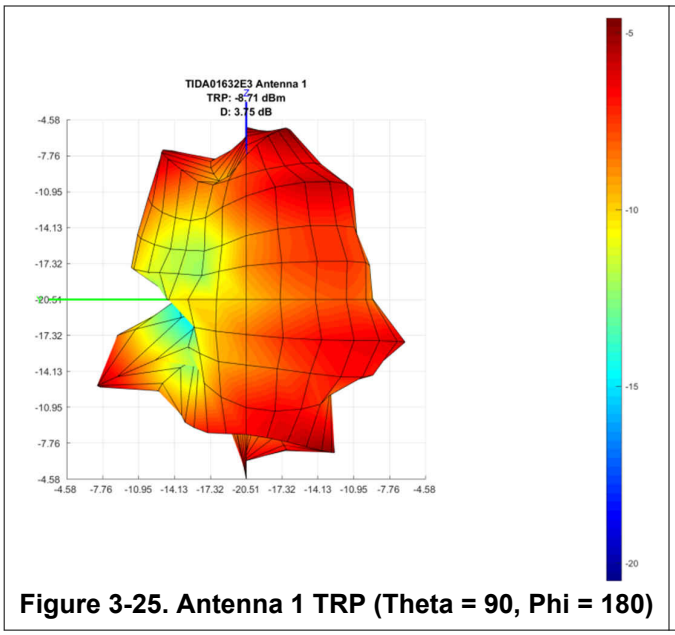

Figure 3-25. Antenna 1 TRP (Theta = 90, Phi = 180)

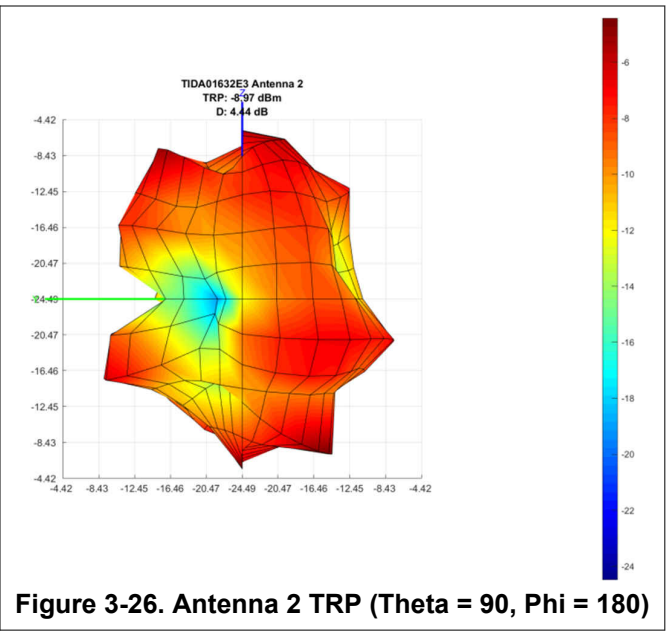

Figure 3-26. Antenna 2 TRP (Theta = 90, Phi = 180)

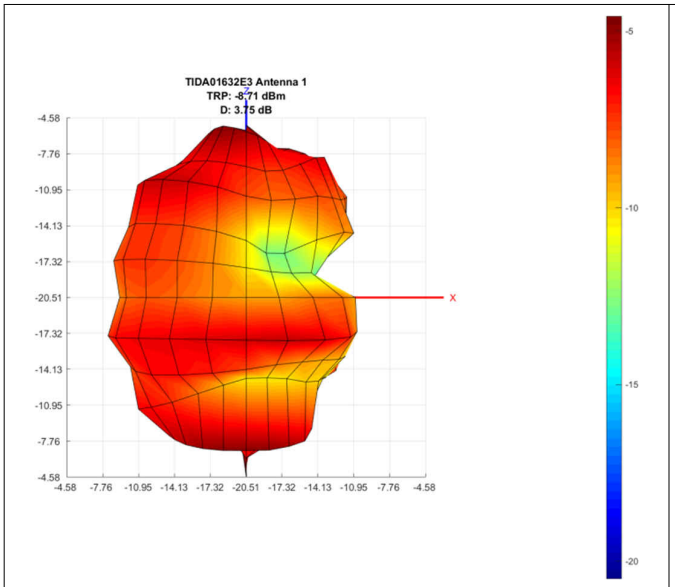

Figure 3-27. Antenna 1 TRP (Theta = 90, Phi = 270)

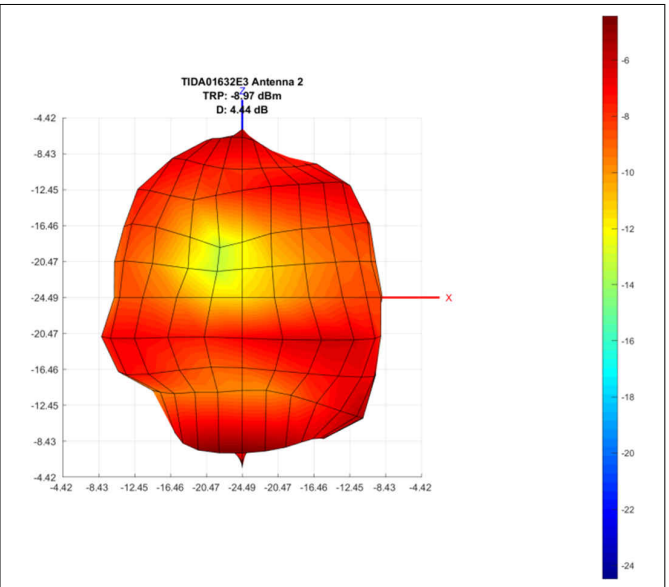

Figure 3-28. Antenna 2 TRP (Theta = 90, Phi = 270)

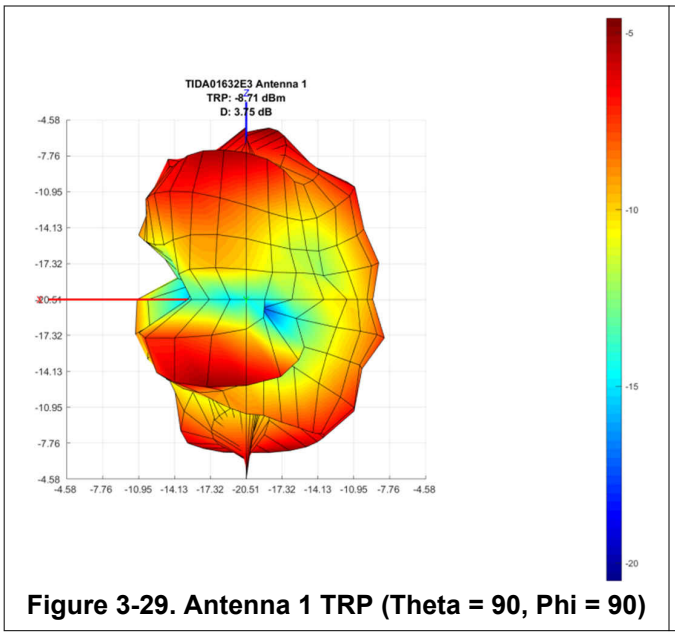

Figure 3-29. Antenna 1 TRP (Theta = 90, Phi = 90)

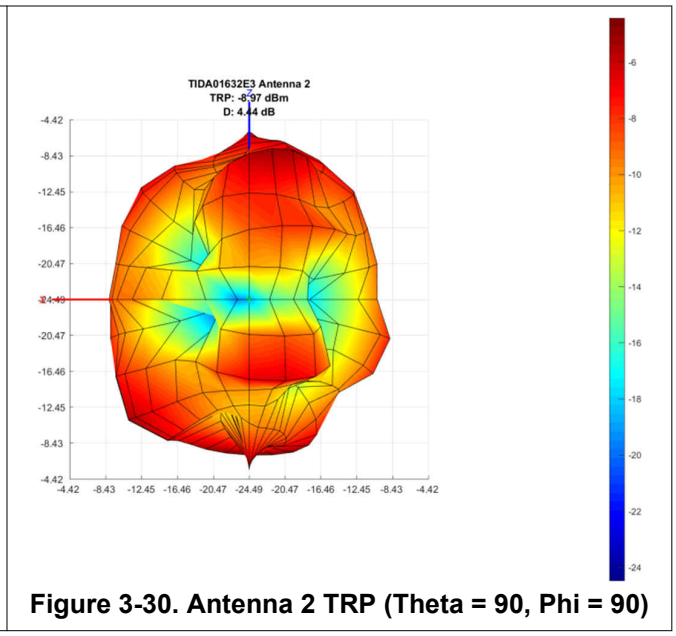

Figure 3-30. Antenna 2 TRP (Theta = 90, Phi = 90)

The TRP was also measured with the TIDA-01632 PCB mounted on a metal stand with RF absorbing material (WaveX WX-A-010-12P) and tin plated copper foil (3M 1183) attached between the PCB and the metal stand shown in Figure 3-31. The added metal around the antenna drastically degrades the efficiency but ensures that no RF signals are received from the back side of the PCB. A measured TRP of around –23 dBm indicates an antenna efficiency of just 0.5%.

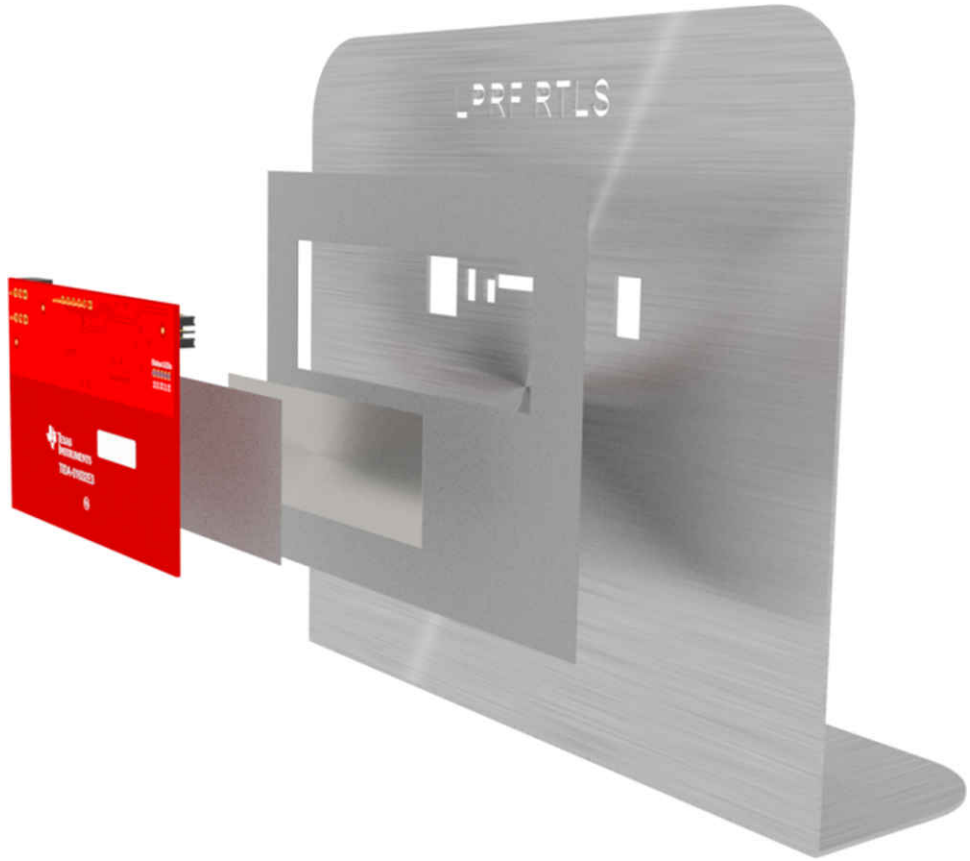

Figure 3-31. PCB + RF Absorbing Material + Tin-Platted Copper Foil + Metal Stand

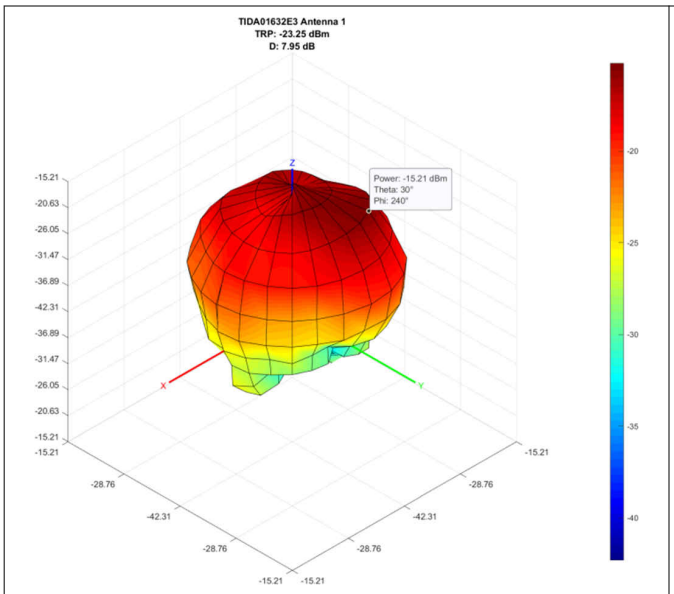

Figure 3-32. PCB + RF Absorbing Material + Tin-Platted Copper Foil + Metal Antenna 1 TRP

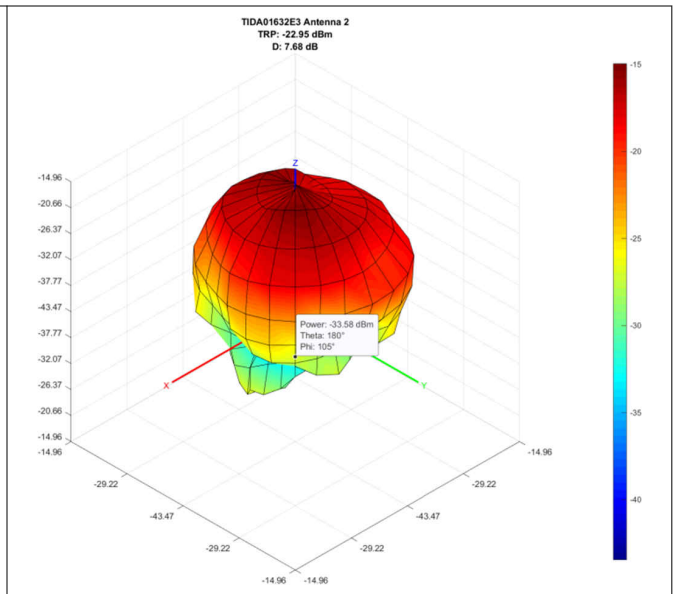

Figure 3-33. PCB + RF Absorbing Material + Tin-Platted Copper Foil + Metal Antenna 2 TRP

3.4.2 Measuring Antenna 1 and 2 Phase Difference

To measure the phase difference between antenna 1 and antenna 2 across –90° to 90°, the turntable (Figure 3-13) was turned from –90° to 90° in 1° increments. I/Q data was collected at each angle, referenced as Phi, from 4 AoA packets at every Bluetooth Low Energy channel. This includes all 40 channels from 2402 MHz to 2480 MHz for a total of 160 AoA packets per angle. Figure 3-34 shows the setup.

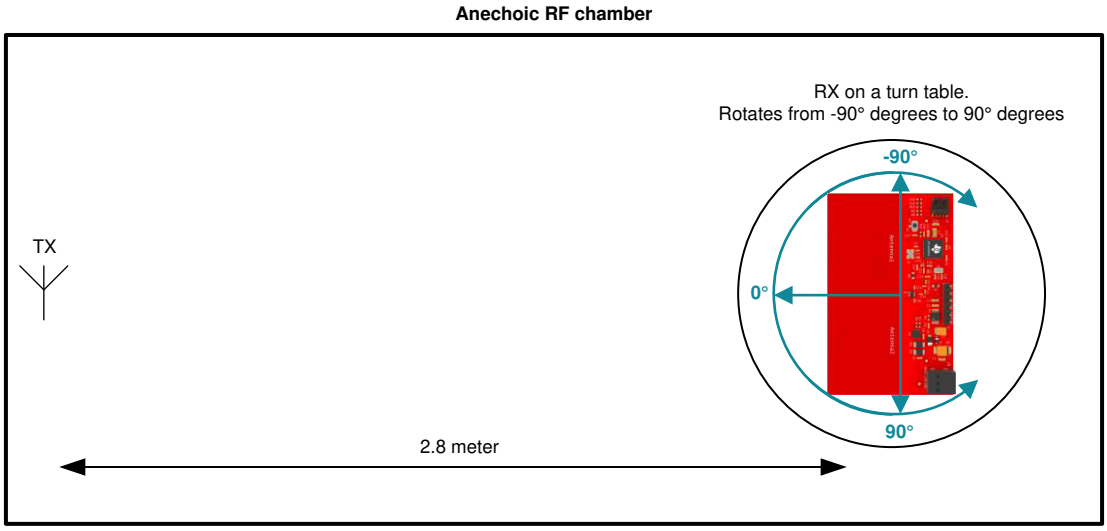

Figure 3-34. Phase Difference Measurement Test Setup

The TIDA-01632 reference design is set up to collect IQ data in 4-µs time-slots from each antenna. The sampling rate is set to 4 MSPS which provides 16 IQ samples per time-slot.

There are various methods and approaches that can be used for AoA estimation. In this application report, the phase difference between two antennas is used to calculate the AoA. Because the AoA tone that is captured has a period equal to the time-slot period (250- KHz tone = 4-µs period), the phases of the same sample number between time-slots can be compared and the phase difference calculated. To calculate the phase difference between two IQ samples (one IQ sample per antenna), the sample from the first antenna is multiplied with the complex conjugate of the sample from the second antenna.

$$x_0 = r_0 e^{i\alpha_0} \quad (1)$$

$$x_1 = r_1 e^{i\alpha_1} \quad (2)$$

$$\text{Angle} = r_0 r_1 e^{i(\alpha_0 - \alpha_1)} = \left(x_0 \times x_1^*\right) \quad (3)$$

In the equations α represents the phase and r represents the magnitude in Equation 1 to Equation 3. Note that the first 8 samples in each time slot are discarded due to antenna switching and settling time so only sample 8 to 15 in each slot are used. See the *BLE-Stack User's Guide: RTLS Toolbox - AoA* for more information on the calculation.

Section 3.4.2.1 through Section 3.4.2.4 show the test results from 4 different hardware setups using the TIDA-01632 PCB. The y-axis on the graphs show the average phase difference between antennas 1 and 2 while the x-axis shows the angle the PCB is facing from the transmitting antenna. The more yellow the trace the lower the frequency, the more red the trace the higher the frequency, and middle frequencies appear as orange traces. When looking at the results from each test setup, the better results have the most linear data.

3.4.2.1 Bare PCB

The first test only involved the bare TIDA-01632 PCB shown in Figure 3-35.

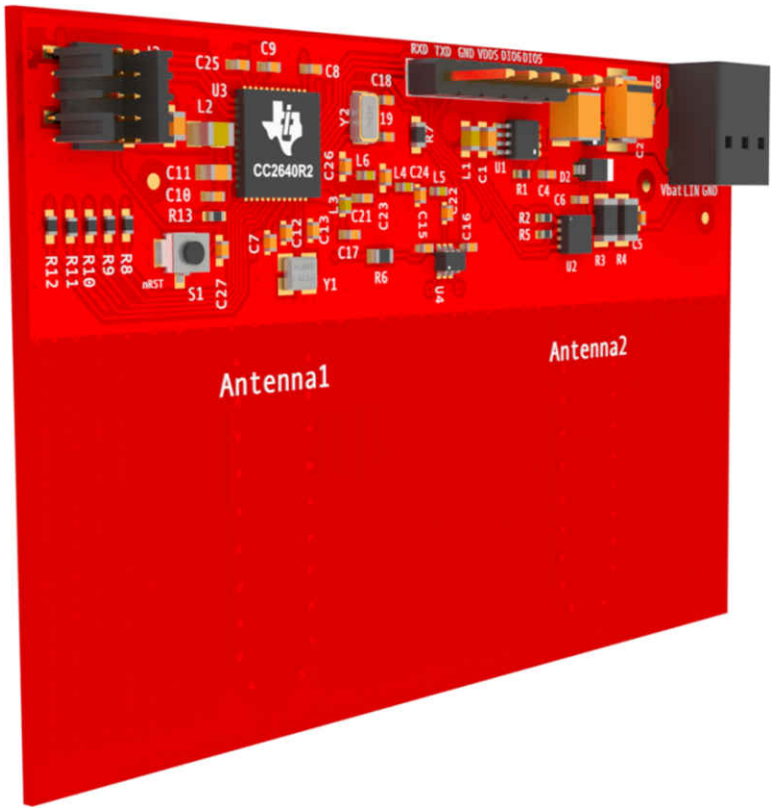

Figure 3-35. Bare PCB

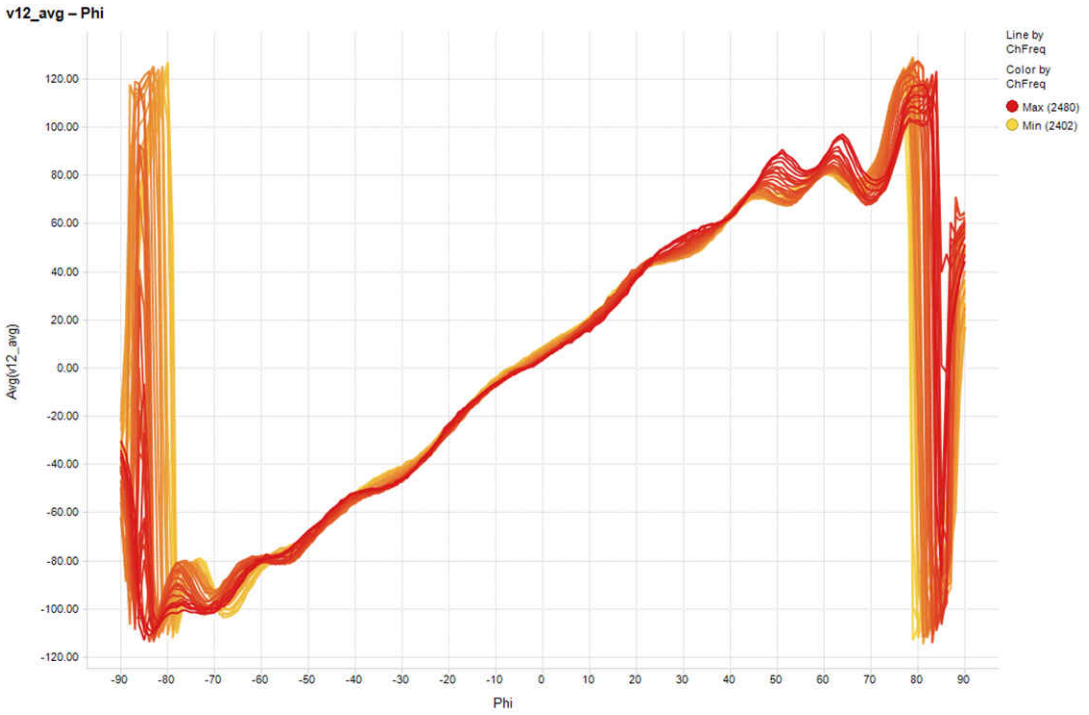

Figure 3-36. Bare PCB Phase Difference Over Angle Results

The bare PCB shows fairly linear results from –60 to 60 degrees with much more error outside of that range. This is a good start to calculating an accurate AoA.

3.4.2.2 PCB + RF Absorbing Material

In this setup, one layer of WaveX WX-A-010-12P RF absorbing material from ARC Technologies is attached on the TIDA-01632 board (on the opposite side from the incoming RF signal) shown in Figure 3-37 and Figure 3-38.

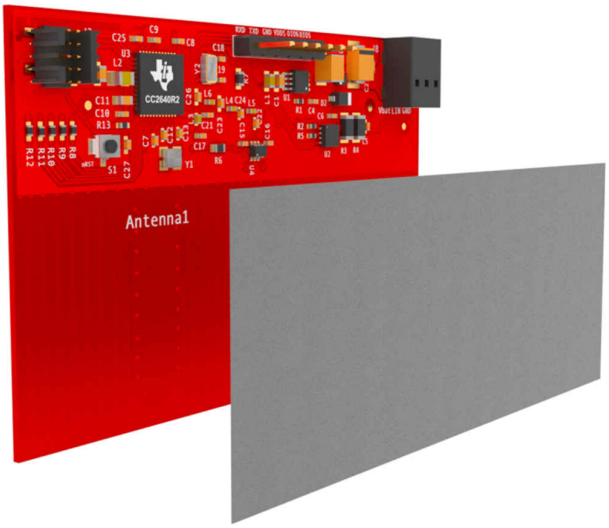

Figure 3-37. PCB + RF Absorbing Material Detached

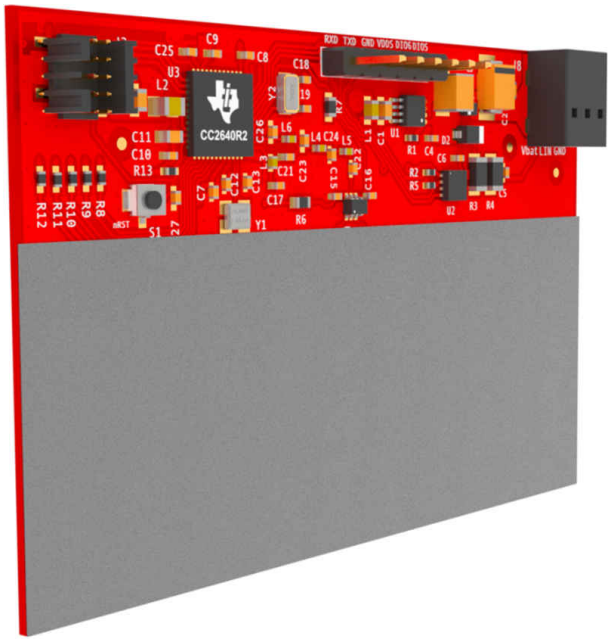

Figure 3-38. PCB + RF Absorbing Material Attached

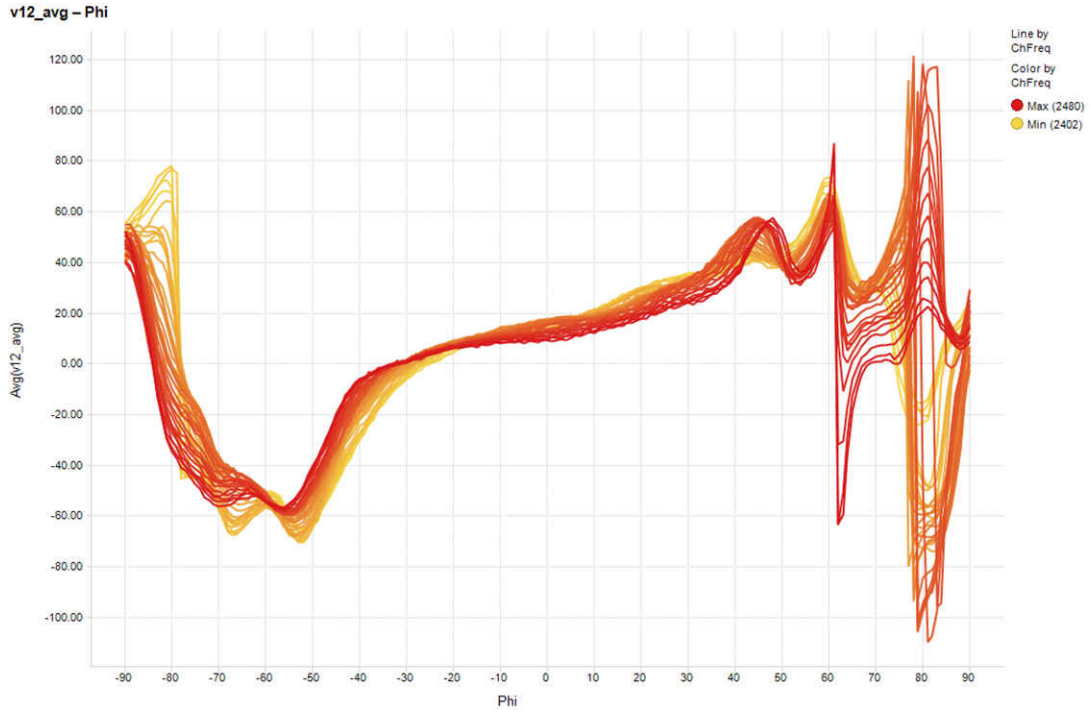

Figure 3-39. PCB + RF Absorbing Material Phase Difference Over Angle Results

The RF absorbing material alone does not improve the measurements and is not recommended for final implementation.

3.4.2.3 PCB + RF Absorbing Material + Tin-Plated Copper Foil

In this setup, one layer of WaveX WX-A-010-12P RF absorbing material from ARC Technologies and one layer of 3M® 1183 tin-plated copper foil is attached on the TIDA-01632 boards (opposite side from the incoming RF signal) shown in Figure 3-40 and Figure 3-41.

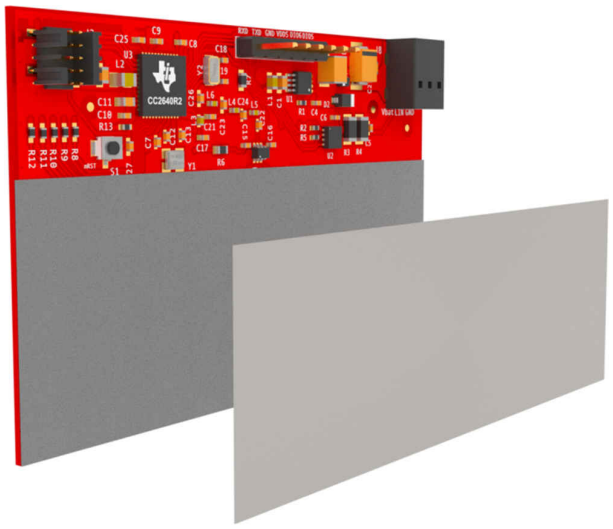

Figure 3-40. PCB + RF Absorbing Material + Tin-Plated Copper Foil Detached

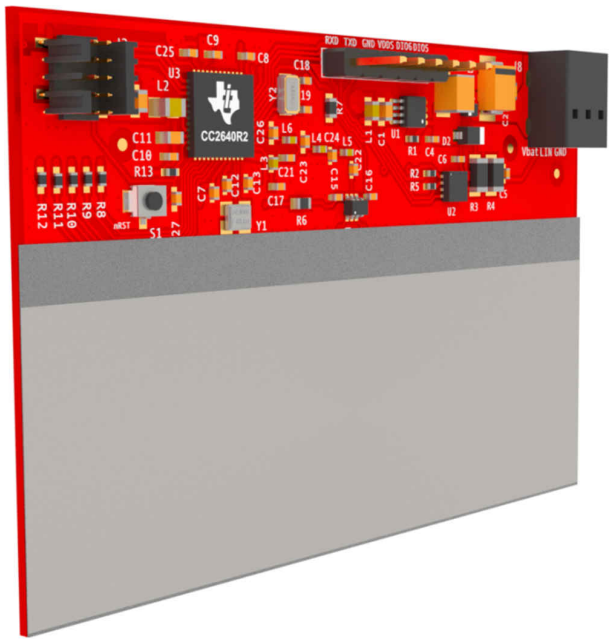

Figure 3-41. PCB + RF Absorbing Material + Tin-Plated Copper Foil Attached

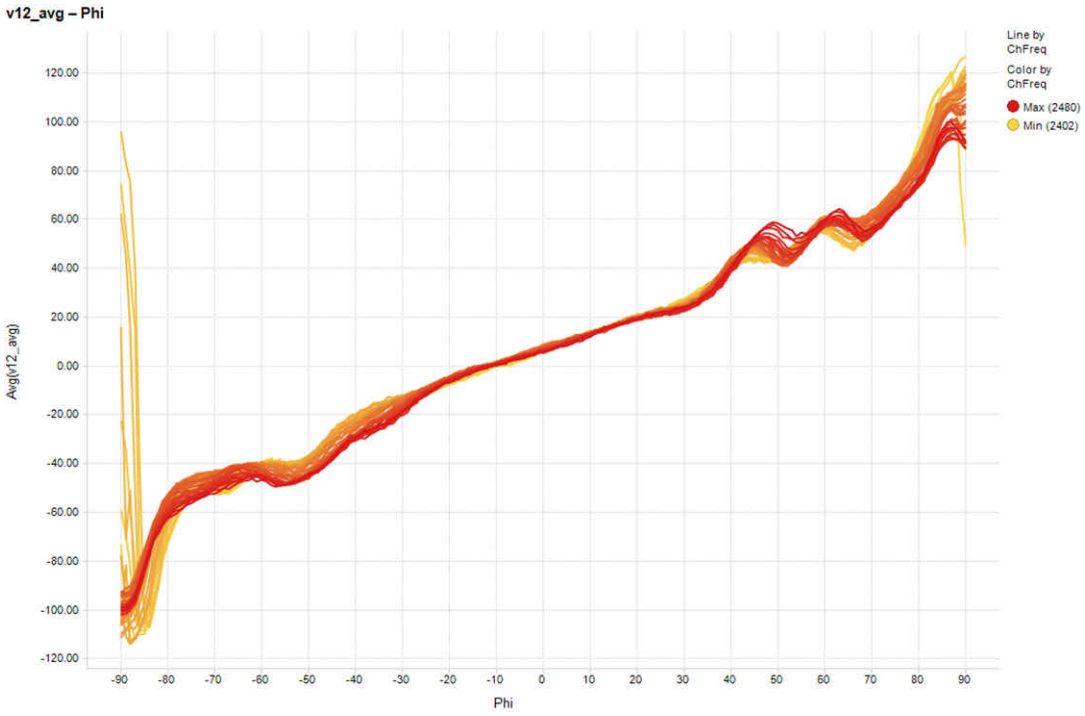

Figure 3-42. PCB + RF Absorbing Material + Tin-Plated Copper Foil Phase Difference Over Angle Results

The tin-platted copper greatly improves the results from the hardware setup with only the RF absorbing material. Also, the wider angle phase difference error is reduced compared to the bare PCB as well showing a range of –75° to 75° with some error.

3.4.2.4 PCB + RF Absorbing Material + Tin-Plated Copper Foil + Metal

In this setup, one layer of WaveX WX-A-010-12P RF absorbing material from ARC Technologies and one layer of 3M 1183 tin-plated copper foil and a metal stand is attached on the TIDA-01632 boards (opposite side from the incoming RF signal) shown in Figure 3-43 and Figure 3-44.

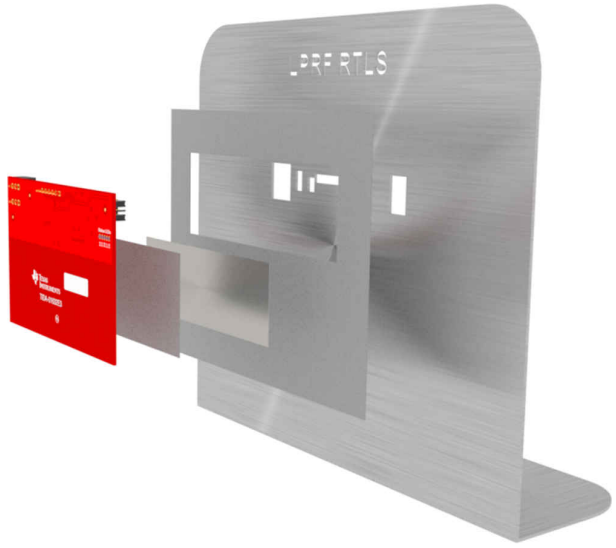

Figure 3-43. PCB + RF Absorbing Material + Tin-Plated Copper Foil + Metal Individual Pieces

Figure 3-44. PCB + RF Absorbing Material + Tin-Plated Copper Foil + Metal

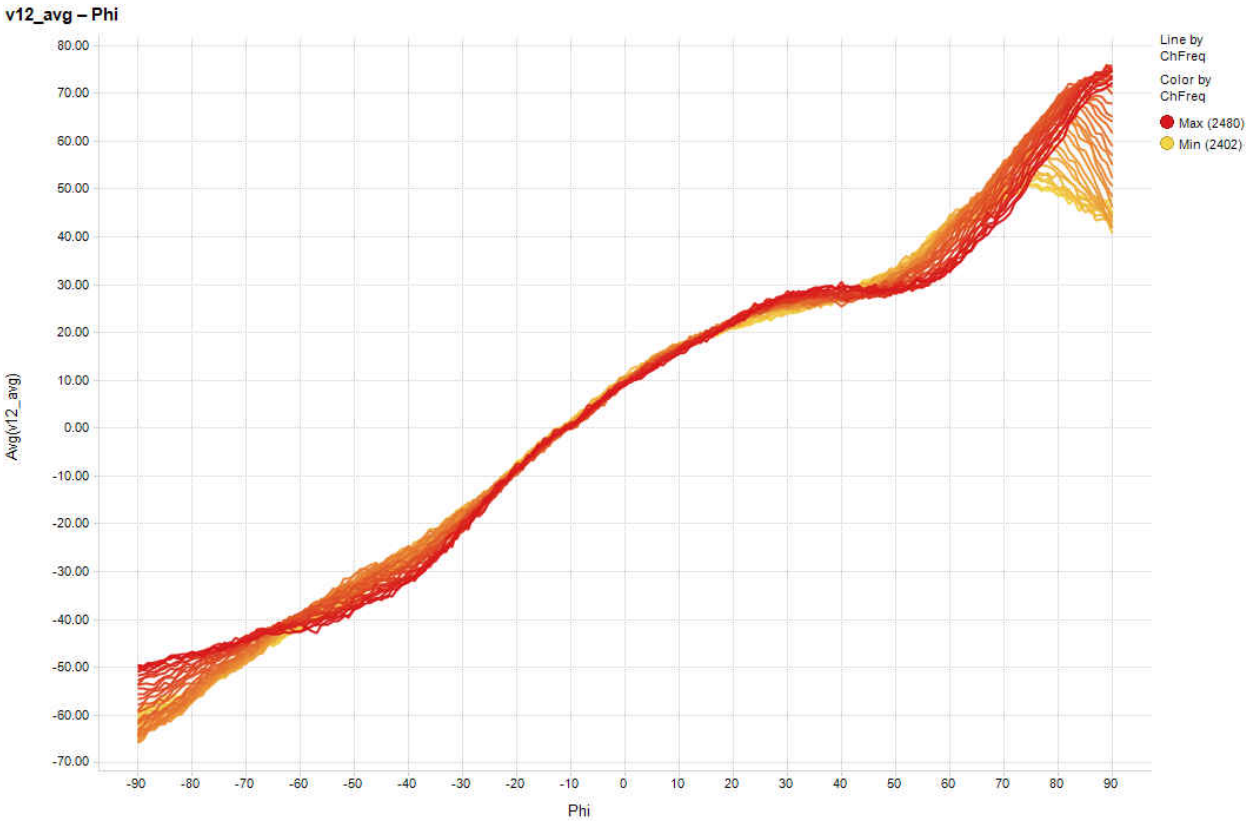

Figure 3-45. PCB + RF Absorbing Material + Tin-Plated Copper Foil + Metal Phase Difference Over Angle Results

The final hardware setup shows the best results over all angles. However, the results are not as linear as the previous setups and show more error outside of the –25° to 25° range.

3.4.3 Phase Difference vs Distance

In an ideal world, the phase difference would be the same for a specific angle over all distances. To test this, the bare PCB phase difference was measured with increasing distance (reducing the transmitting antenna signal strength). Figure 3-46 shows the results.

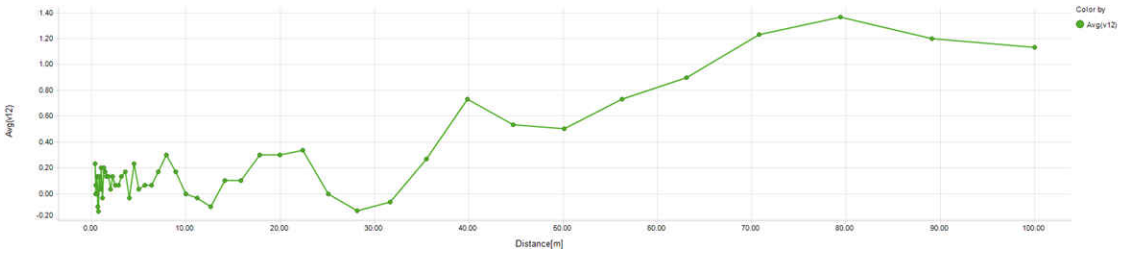

Figure 3-46. Phase Difference vs Distance

Notice that the variance does not exceed 0.40° until the distance is greater than approximately 35 m.

4 Calculating AoA From IQ Measurements

In Section 3, the measured phases were used to calculate a phase difference between the two antennas with different hardware setups. The next step is to calculate AoA based on the measured phase difference. With a known spacing between the antennas (d), and phase difference between the two antennas measured (Φ), the AoA can be calculated using simple trigonometry as Figure 4-1 shows.

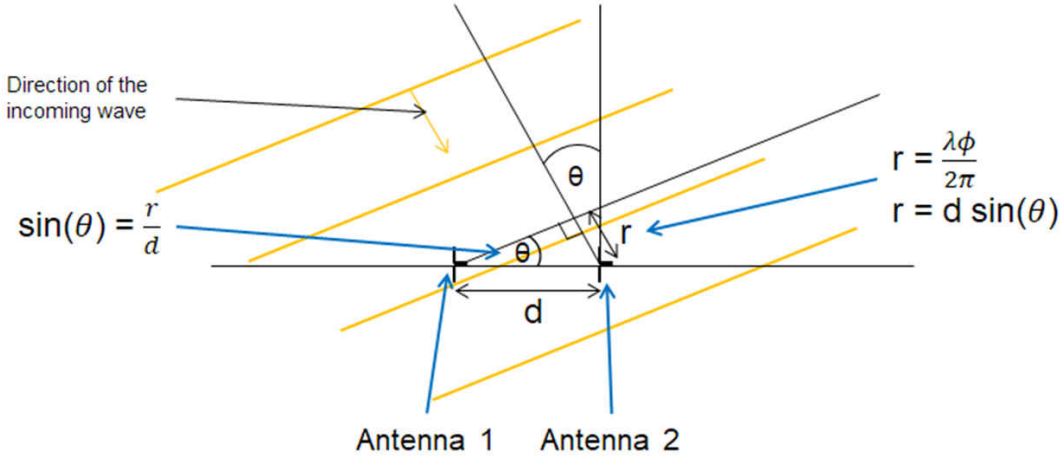

Figure 4-1. AoA Equations

The equations in Figure 4-1 can be simplified to Equation 4.

$$\theta = \sin^{-1}\frac{\lambda f}{2\pi d} \tag{4}$$

Note that r is the distance to antenna 2 that the incident wave needs to travel after arriving at antenna 1. Because the phase difference is known (Φ), the extra distance r is equal to the wavelength of the incoming signal times Φ / (2π). For more information on the AoA calculation, see the *SimpleLink Academy -> RTLS Toolbox -> Angle of Arrival (AoA)*. Performing the arcsin() function using the wavelength, known antenna phase center spacing, and calculated phase difference between the two antennas, the AoA is calculated.

After the AoA is calculated, the value may need to be compensated due to variation in results across frequency and antenna design. Therefore, a constant gain, an offset, or both may be used to improve the AoA results.

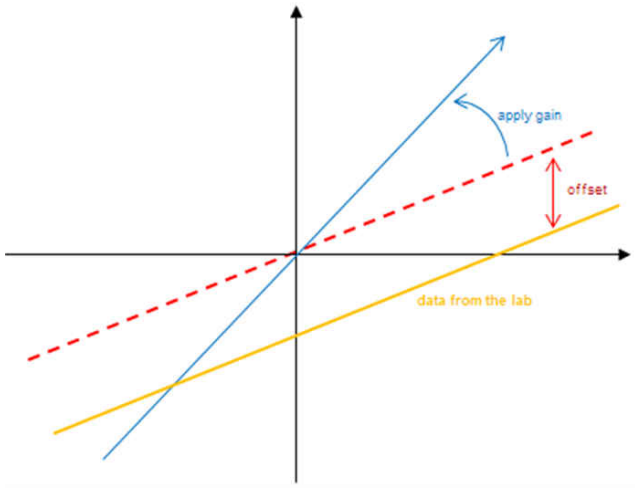

Figure 4-2. Compensation to Linear Plot

For more information on AoA compensation, see the *Angle Compensation* section of the *SimpleLink™ CC2640R2 SDK BLE-Stack User's Guide*.

4.1 Dipole Antenna Array Uncompensated Angle of Arrival Results

Using Equation 4, the angle of arrivals were calculated and plotted. Similar to the graphs in Section 3.4.2, the x-axis, Phi, is the actual angle the PCB was facing the transmitter and the y-axis is the average of the multiple calculated angle of arrivals from the multiple phase measurements. In addition, the lower the frequency the more yellow the trace and the higher the frequency the more red. The desired result shows the calculated AoA equal to Phi and the graphs display a perfect line showing that Phi equals AoA for all frequencies. This line is referenced on all AoA vs Phi graphs.

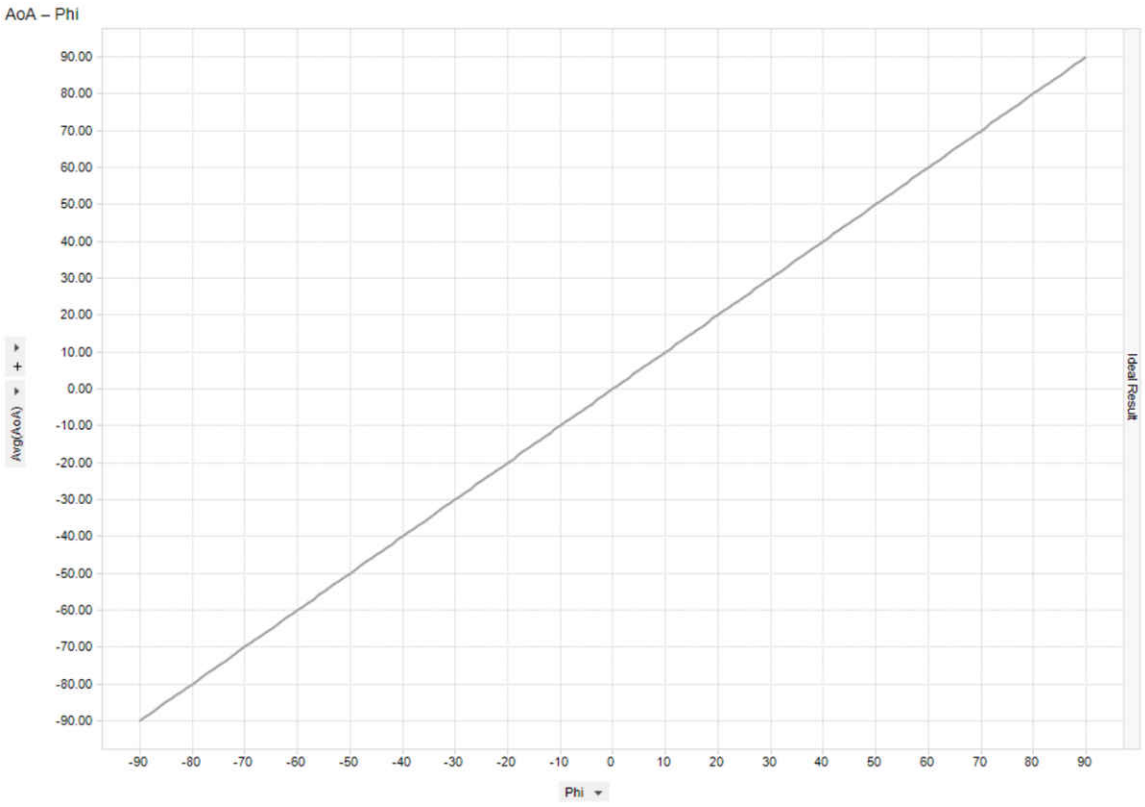

Figure 4-3. Ideal AoA Result

Figure 4-4 shows the results of all four different setups, with the bare PCB at the top, PCB + RF absorbing material second, PCB + RF absorbing material + tin-plated copper foil third, and PCB + RF absorbing material + tin-plated copper foil + metal at the bottom.

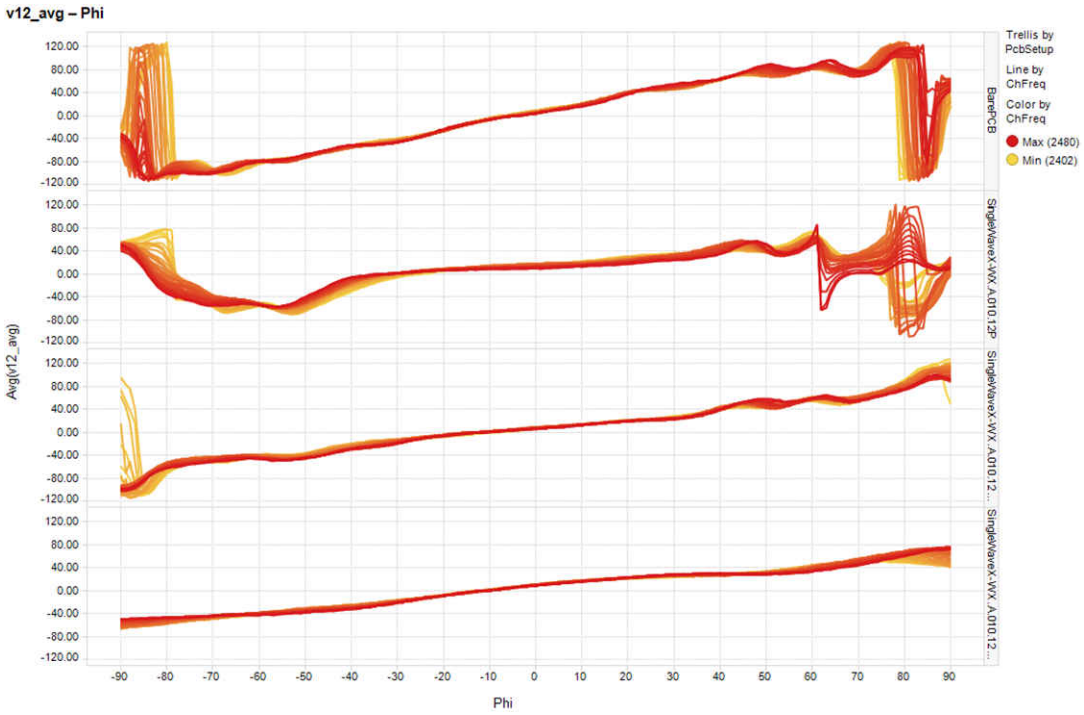

Figure 4-4. All Hardware AoA Results Over all Bluetooth Low Energy Channels

The bare PCB is the closest to measuring the true AoA but has large error as the angles get closer to ±90°. However, the PCB + RF absorbing material + tin-plated copper foil + metal setup has the most linear results at the widest angles. Figure 4-5 shows the error from the calculated AoA and the actual angle Phi.

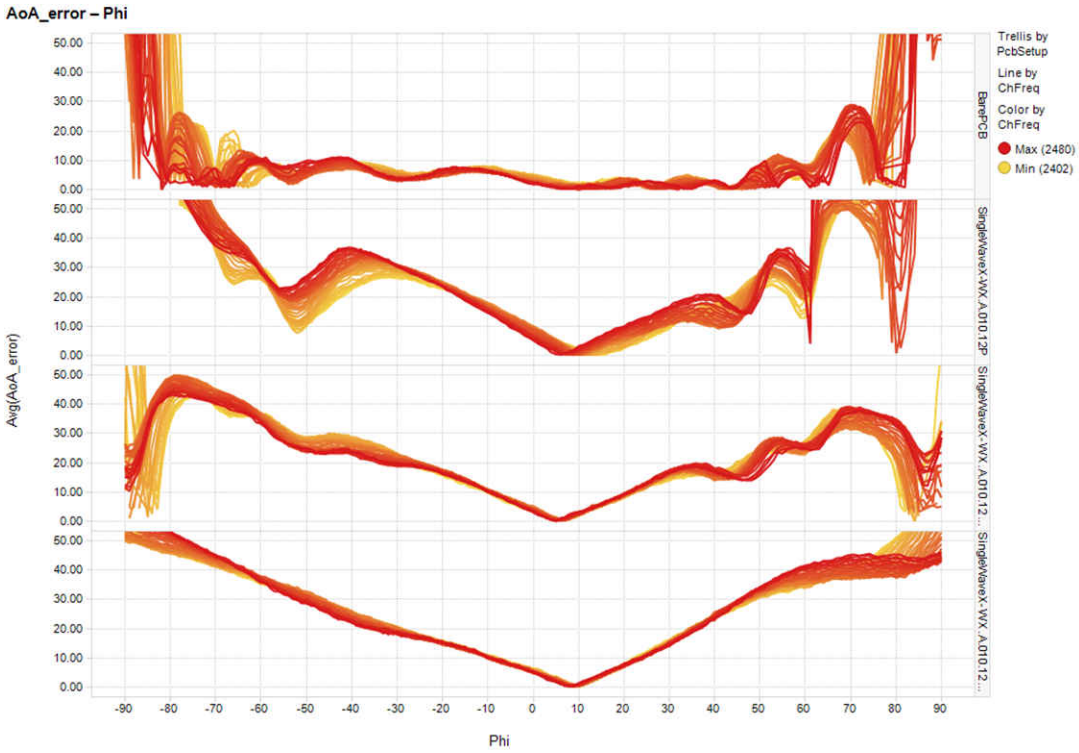

Figure 4-5. All Hardware AoA Error Results Over all Bluetooth Low Energy Channels

When interpreting the data, it is good to see consistent error as this can be compensated for as shown in Section 4.2. Notice that the PCB + RF absorbing material + tin-plated copper foil + metal has the most consistent error but needs compensation to improve the overall performance. With no compensation, the bare PCB shows the least error and most accurate results. The following subsections focus on the uncompensated AoA results for each test setup vs the actual AoA.

4.1.1 Bare PCB Uncompensated AoA

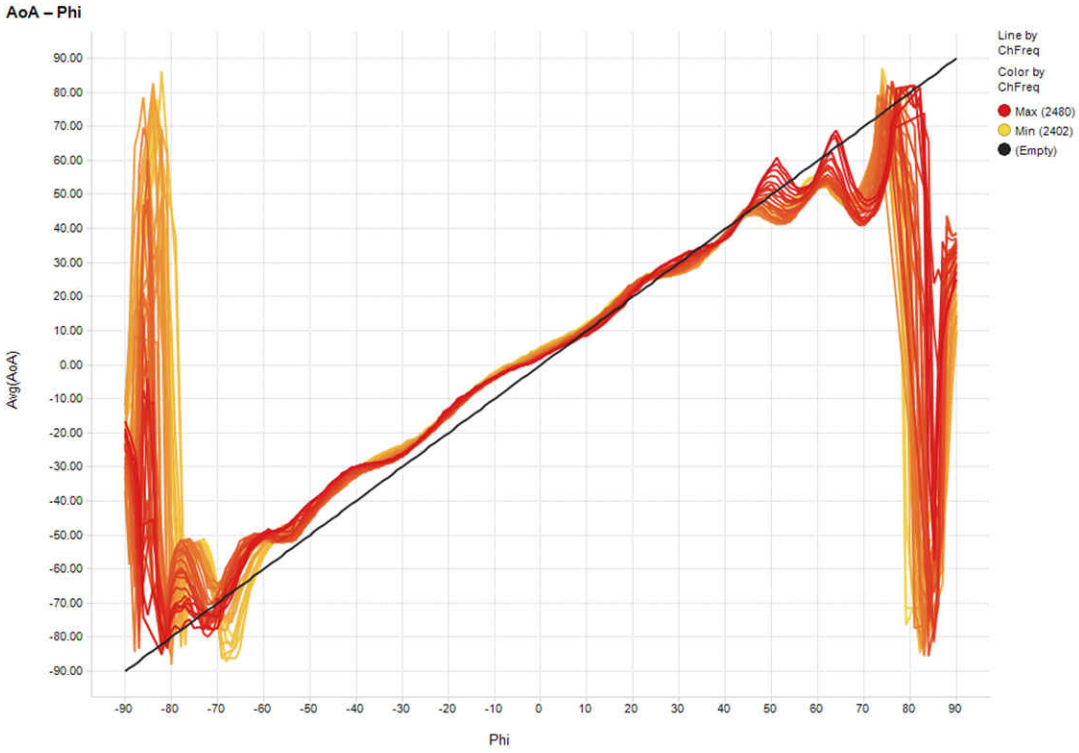

Figure 4-6. Bare PCB Uncompensated AoA Results Over all Bluetooth Low Energy Channels

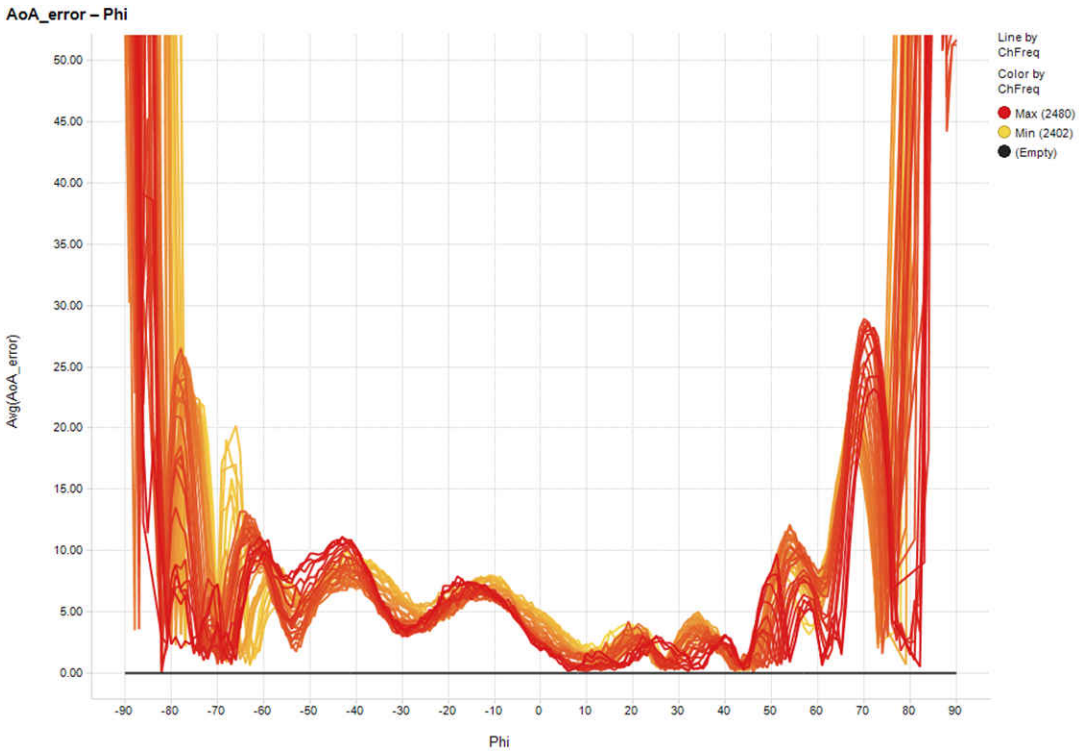

Figure 4-7. Bare PCB Uncompensated AoA Error Results

4.1.2 PCB + RF Absorbing Material Uncompensated AoA

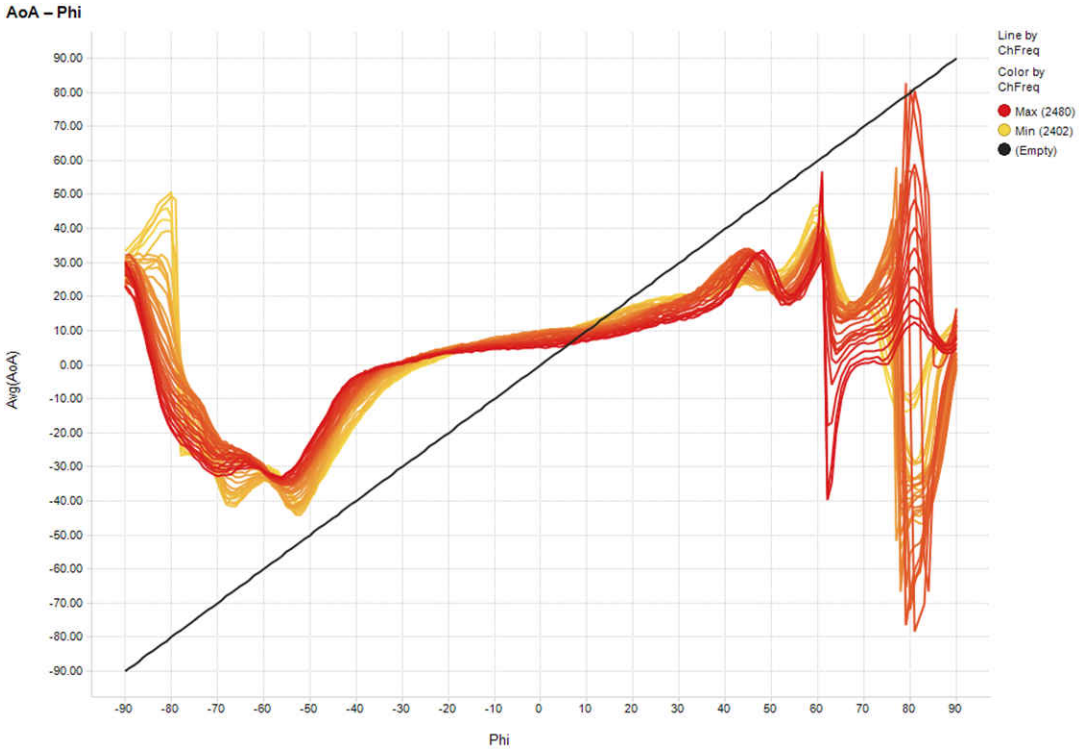

Figure 4-8. PCB + RF Absorbing Material Uncompensated AoA Over all Bluetooth Low Energy Channels

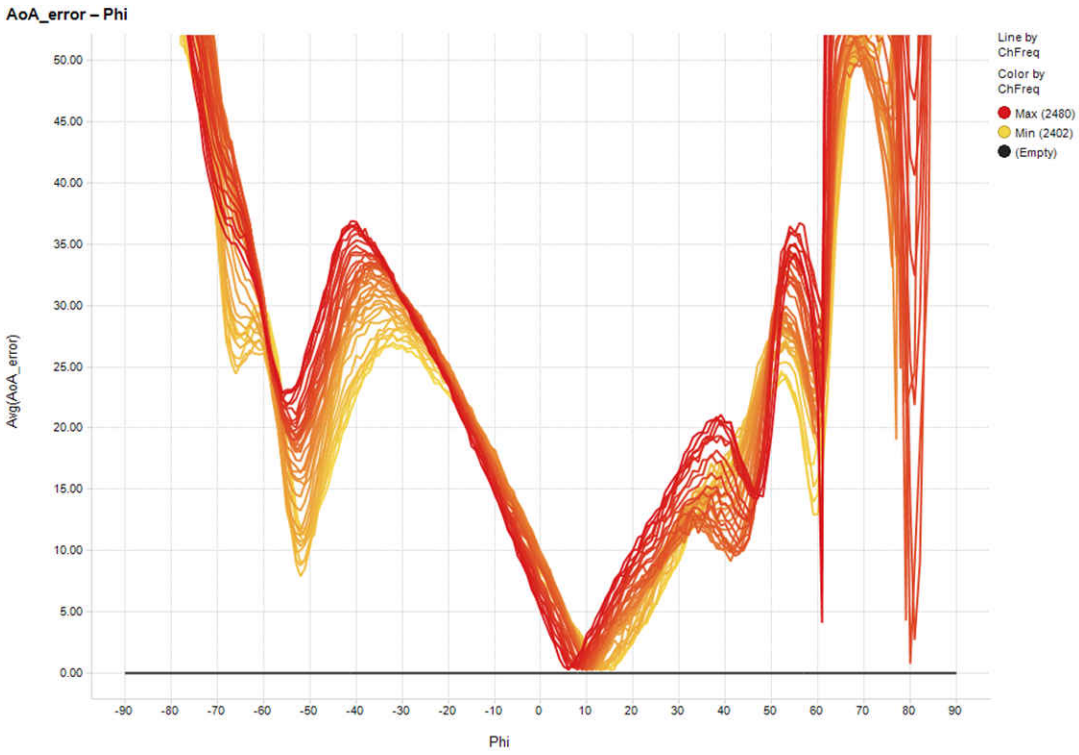

Figure 4-9. PCB + RF Absorbing Material Uncompensated AoA Error

4.1.3 PCB + RF Absorbing Material + Tin-Plated Copper Foil Uncompensated AoA

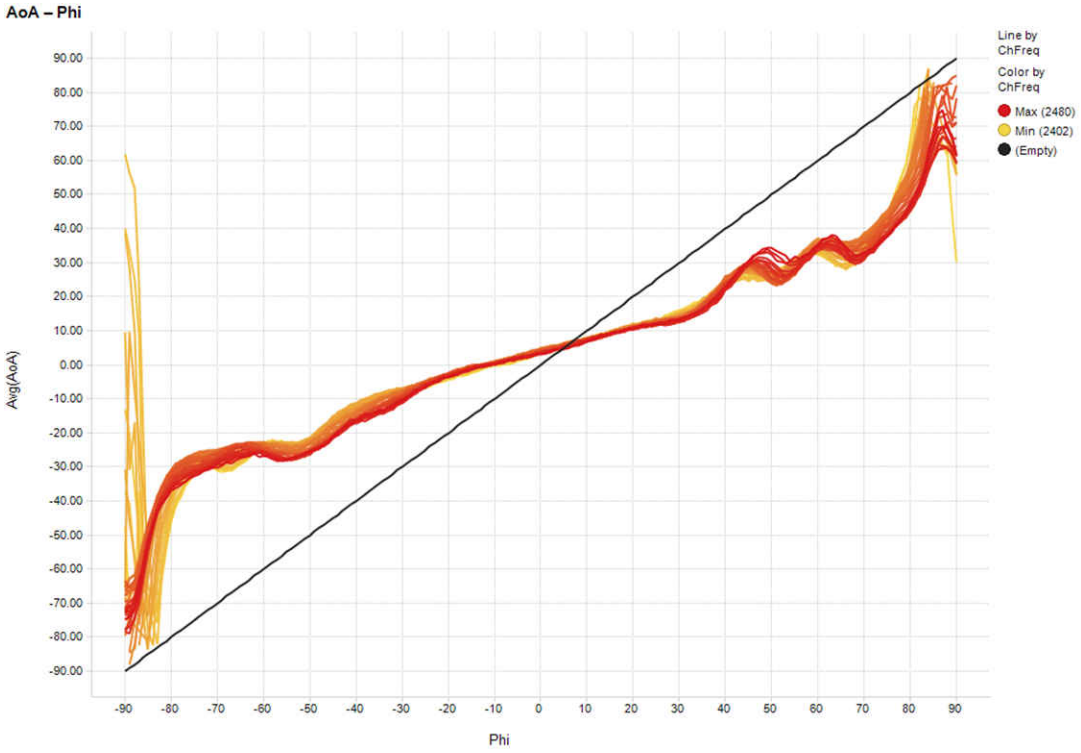

Figure 4-10. PCB + RF Absorbing Material + Tin-Plated Copper Foil Uncompensated AoA Results Over all Bluetooth Low Energy Channels

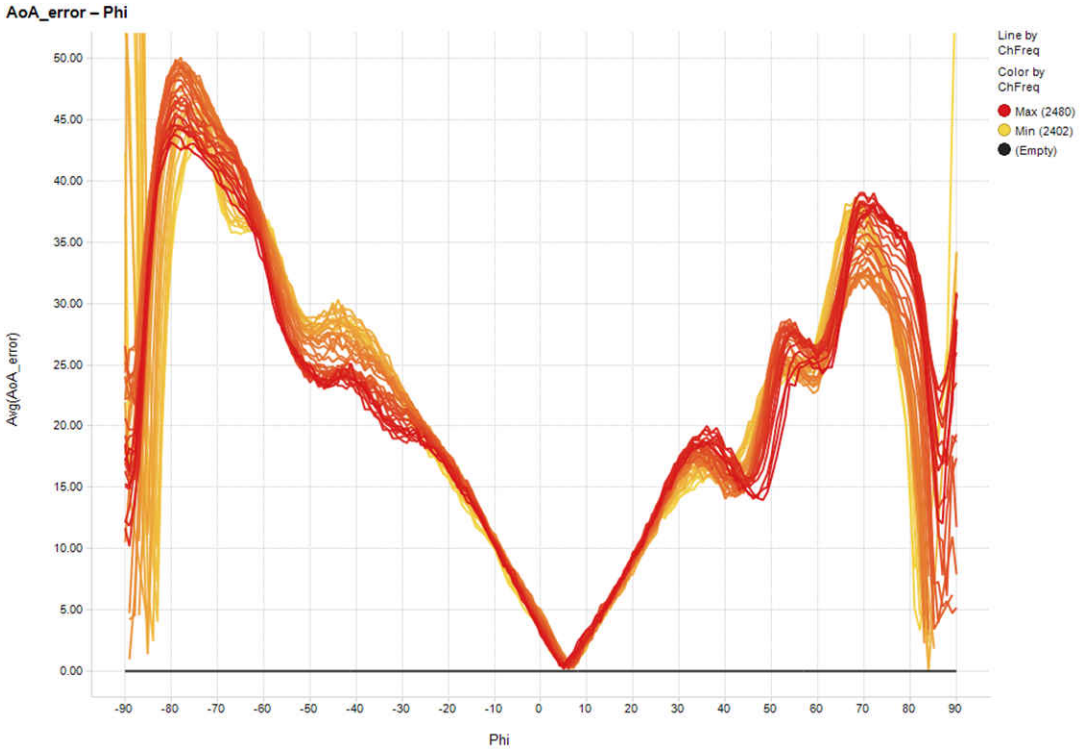

Figure 4-11. PCB + RF Absorbing Material + Tin-Plated Copper Foil Uncompensated AoA Error

4.1.4 PCB + RF Absorbing Material + Tin-Plated Copper Foil + Metal Uncompensated AoA

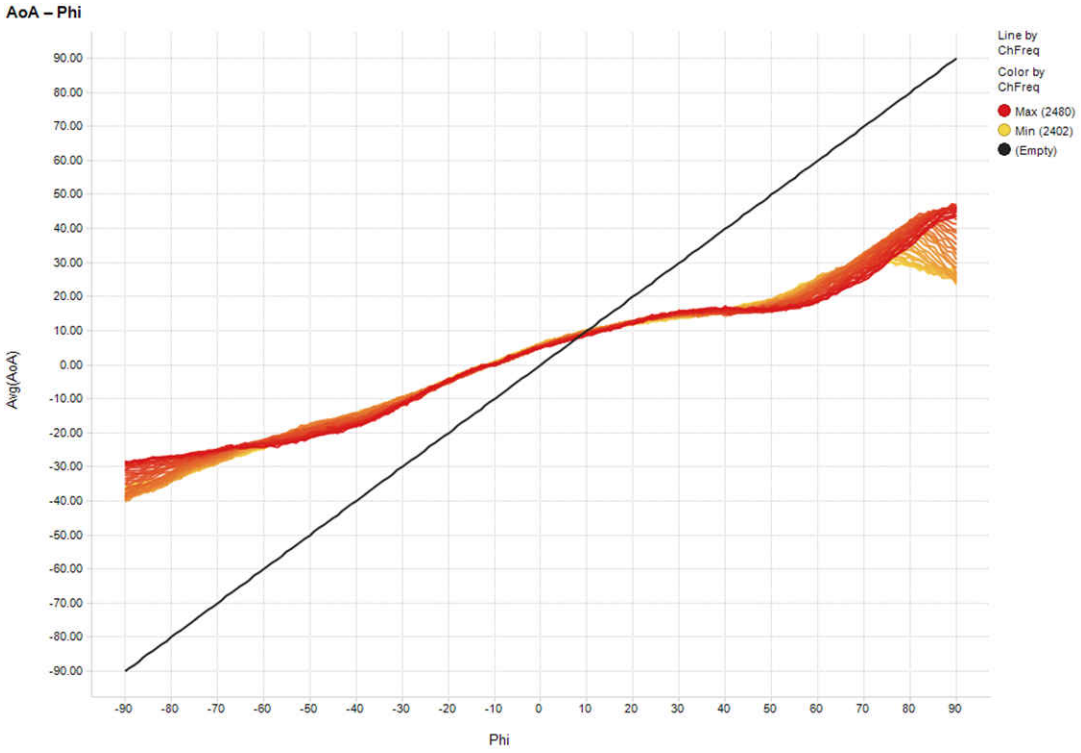

Figure 4-12. PCB + RF Absorbing Material + Tin-Plated Copper Foil + Metal Uncompensated AoA Results Over all Bluetooth Low Energy Channels

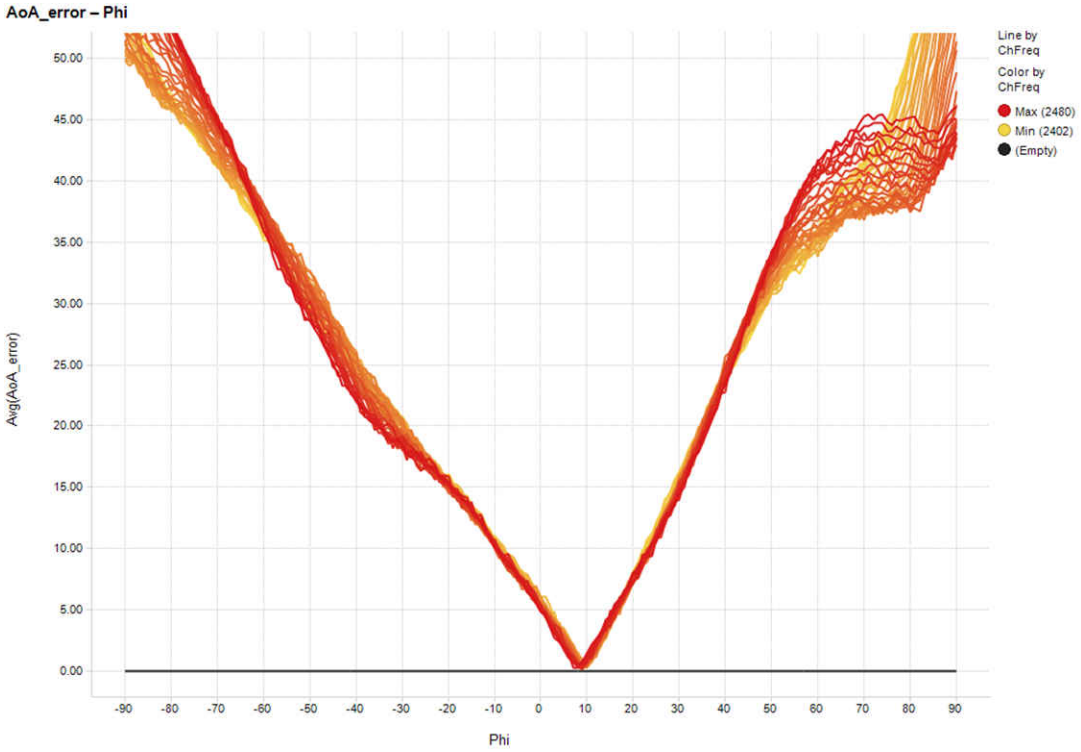

Figure 4-13. PCB + RF Absorbing Material + Tin-Plated Copper Foil + Metal Uncompensated AoA Error

4.2 Dipole Antenna Array Compensated AoA Results

In this section, gain and offset compensation is added to the base calculated AoA values in Section 4.1 (excluding the PCB + RF absorbing material hardware setup) to reduce the AoA error from the actual angle Phi. The compensation is applied as Equation 5 shows.

$$AoA_{Comp} = (\theta + b) \times m \tag{5}$$

where

- θ equals the calculated AoA
- b equals the offset
- m equals the gain

For all hardware setups except the setup with the metal stand, the offset value was selected to make sure that when Phi equals zero, the calculated average AoA also equals zero. This offset was adjusted for each individual frequency as all frequencies require a slightly different offset value. To calculate the gain, the best fit line method was used for each frequency in the most linear range (that is, –65° to 65°) after adding the required offset. However, there is much smaller variance of gain values over frequency as the majority of frequencies require the same gain or similar gain values.

4.2.1 Bare PCB AoA With Compensation

The bare PCB required the least amount of compensation as the results were fairly close to Phi. However, Table 4-1 shows the gain and offset values used for each frequency.

Table 4-1. Bare PCB AoA Compensation Values

Frequency (MHz)	Channel	Gain	Offset
2402	37	1.12	–4.69
2404	0	1.12	–4.69
2406	1	1.12	–5.04
2408	2	1.14	–4.82
2410	3	1.14	–4.82
2412	4	1.14	–5.1
2414	5	1.15	–4.81
2416	6	1.15	–4.73
2418	7	1.15	–4.45
2420	8	1.15	–4.73
2422	9	1.15	–4.16
2424	10	1.15	–4.37
2426	38	1.15	–4.22
2428	11	1.15	–4.36
2430	12	1.15	–3.86
2432	13	1.14	–3.65
2434	14	1.14	–3.72
2436	15	1.15	–3.57
2438	16	1.14	–3.43
2440	17	1.14	–3.29
2442	18	1.14	–2.93
2444	19	1.12	–3
2446	20	1.12	–2.09
2448	21	1.12	–2.79
2450	22	1.12	–2.65
2452	23	1.12	–2.57
2454	24	1.12	–2.64
2456	25	1.12	–2.36
2458	26	1.12	–2.64
2460	27	1.12	–2.36
2462	28	1.12	–2.08
2464	29	1.11	–2.49
2466	30	1.11	–2.35
2468	31	1.11	–2.63
2470	32	1.11	–2.14
2472	33	1.11	–2.55
2474	34	1.11	–2.41
2476	35	1.11	–2.07
2478	36	1.11	–1.86
2480	39	1.09	–1.99

Figure 4-14 shows the uncompensated AoA error vs Phi (the actual angle) and Figure 4-15 the compensated AoA error vs Phi.

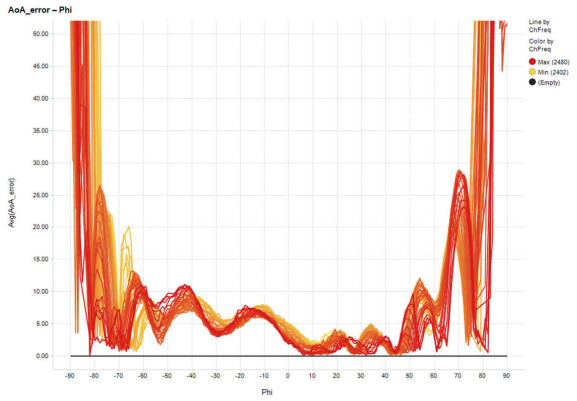

Figure 4-14. Bare PCB Uncompensated AoA Error Results

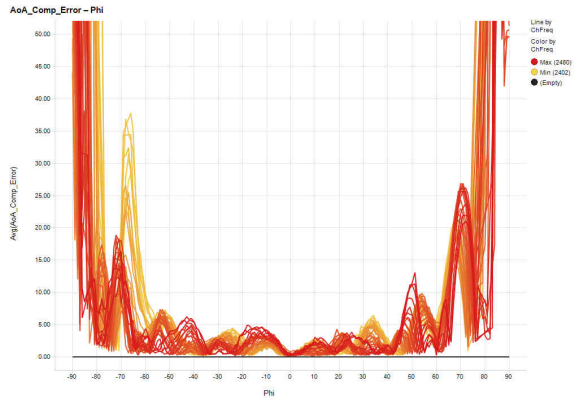

Figure 4-15. Bare PCB Compensated AoA Error Results

It is clear that the error is greatly reduced over the most linear range (–65° to 65°). Figure 4-16 and Figure 4-17 show how the results have been adjusted to follow the ideal AoA vs Phi plot. There is less than 10° of error across the majority of frequencies from –70° to 65°.

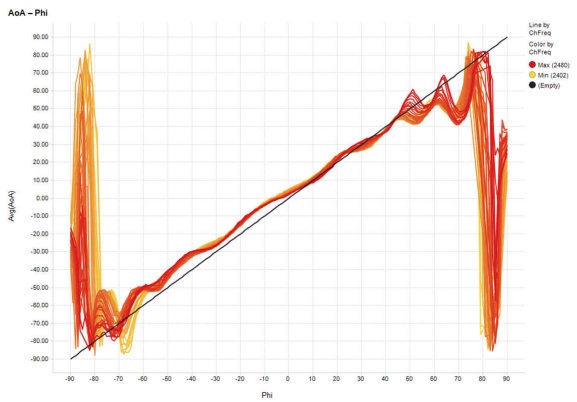

Figure 4-16. Bare PCB Uncompensated AoA Results Over all Bluetooth Low Energy Channels

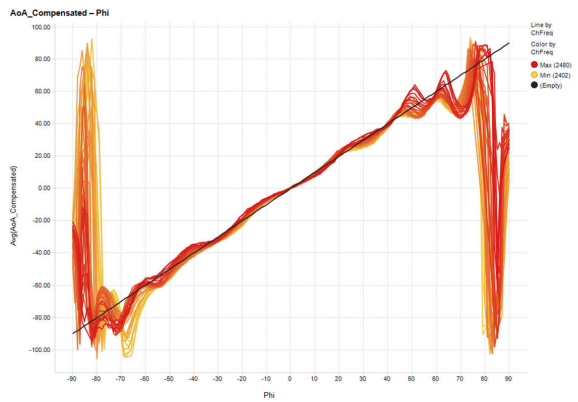

Figure 4-17. Bare PCB Compensated AoA Results Over all Bluetooth Low Energy Channels

4.2.2 PCB + RF Absorbing Material + Tin-Plated Copper Foil Compensated AoA

This hardware setup's initial tests showed fairly linear results. Therefore, with compensation, AoA values are fairly accurate (depending on the frequency) from ±80°. Table 4-2 shows the compensation values used for each frequency.

Table 4-2. PCB + RF Absorbing Material + Tin-Plated Copper Foil AoA Compensation Values

Frequency (MHz)	Channel	Gain	Offset
2402	37	2.17	–3.27
2404	0	2.17	–3.34
2406	1	2.17	–3.48
2408	2	2.17	–3.54
2410	3	2.22	–3.82
2412	4	2.22	–3.54
2414	5	2.22	–4.1
2416	6	2.22	–4.1
2418	7	2.22	–4.02
2420	8	2.22	–4.16
2422	9	2.17	–4.37
2424	10	2.17	–4.44
2426	38	2.17	–4.5
2428	11	2.17	–4.22
2430	12	2.17	–5.06
2432	13	2.17	–4.56
2434	14	2.17	–4.98
2436	15	2.17	–4.2
2438	16	2.17	–4.27
2440	17	2.13	–4.62
2442	18	2.13	–4.61
2444	19	2.17	–4.12
2446	20	2.17	–4.4
2448	21	2.17	–4.39
2450	22	2.17	–4.04
2452	23	2.17	–4.46
2454	24	2.17	–4.17
2456	25	2.17	–4.03
2458	26	2.17	–3.96
2460	27	2.17	–3.75
2462	28	2.17	–3.74
2464	29	2.17	–3.88
2466	30	2.13	–3.6
2468	31	2.13	–3.73
2470	32	2.13	–3.52
2472	33	2.13	–3.52
2474	34	2.13	–3.52
2476	35	2.08	–3.38
2478	36	2.04	–3.24
2480	39	2.04	–3.03

Figure 4-18 shows the uncompensated AoA error vs Phi and Figure 4-19 shows the compensated AoA error vs Phi.

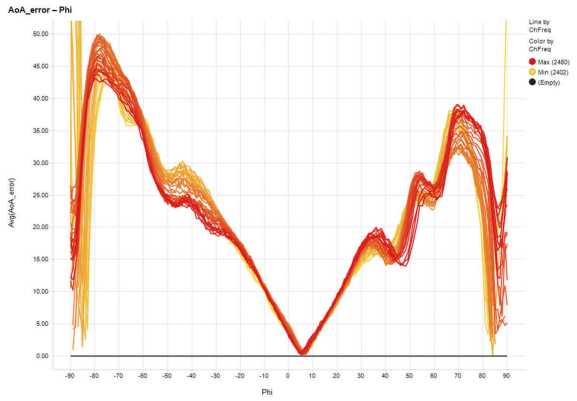

Figure 4-18. PCB + RF Absorbing Material + Tin-Plated Copper Foil Uncompensated AoA Error

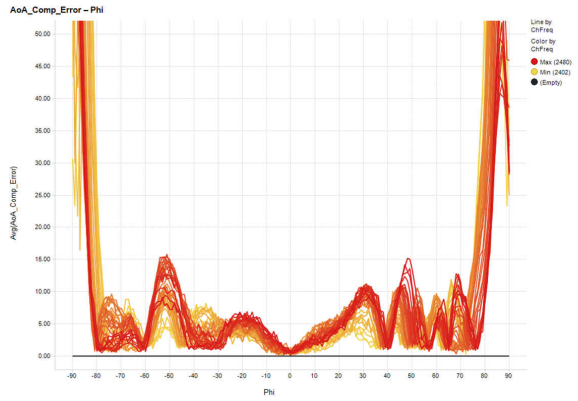

Figure 4-19. PCB + RF Absorbing Material + Tin-Plated Copper Foil Compensated AoA Error

Compensation greatly reduces the AoA error and shows less than 10° of error over most frequencies from –80° to 75°. Figure 4-20 and Figure 4-21 show how the AoA data has been adjusted to be closer to the desired result.

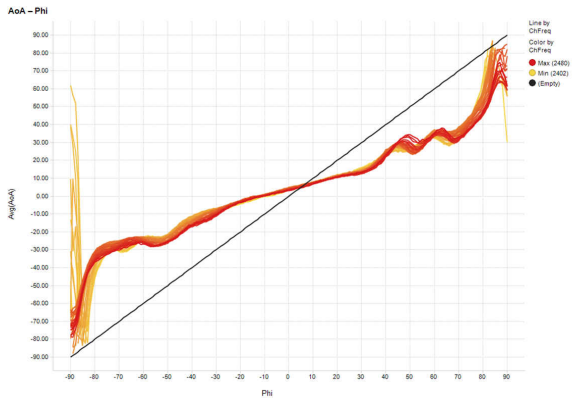

Figure 4-20. PCB + RF Absorbing Material + Tin-Plated Copper Foil Uncompensated AoA Results Over all Bluetooth Low Energy Channels

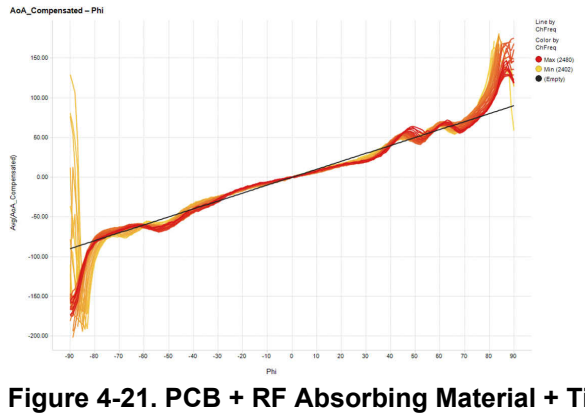

Figure 4-21. PCB + RF Absorbing Material + Tin-Plated Copper Foil Compensated AoA Results Over all Bluetooth Low Energy Channels

4.2.3 PCB + RF Absorbing Material + Tin-Plated Copper Foil + Metal Compensated AoA

The PCB + RF absorbing material + tin-plated copper foil + metal hardware setup is the only hardware setup that the offset was not adjusted for AoA to equal zero when Phi equals 0. The results are not linear for the whole –90° to 90° range and to balance the error across the full angle range, the offset was set to have an error of 7° when Phi equals 0. Better compensation methods can be used to improve the results but in this paper, only basic best fit line linear compensation was implemented. Table 4-3 shows the gain and offset used for each frequency.

Table 4-3. PCB + RF Absorbing Material + Tin-Plated Copper Foil + Metal Compensation Values

Frequency (MHz)	Channel	Gain	Offset
2402	37	2.44	–2.55
2404	0	2.44	–2.12
2406	1	2.44	–2.87
2408	2	2.44	–3.07
2410	3	2.44	–3.16
2412	4	2.44	–3.28
2414	5	2.44	–3.22
2416	6	2.38	–2.71
2418	7	2.38	–2.92
2420	8	2.38	–2.92
2422	9	2.38	–2.21
2424	10	2.38	–3.15
2426	38	2.38	–2.55
2428	11	2.38	–2.68
2430	12	2.38	–3.11
2432	13	2.38	–2.82
2434	14	2.38	–2.74
2436	15	2.38	–2.74
2438	16	2.38	–2.66
2440	17	2.38	–2.44
2442	18	2.38	–2.37
2444	19	2.44	–2.65
2446	20	2.44	–2.37
2448	21	2.44	–2.62
2450	22	2.44	–2.5
2452	23	2.5	–2.68
2454	24	2.5	–2.35
2456	25	2.5	–2.4
2458	26	2.5	–2.62
2460	27	2.56	–2.4
2462	28	2.56	–2.33
2464	29	2.56	–2.53
2466	30	2.63	–2.66
2468	31	2.63	–2.32
2470	32	2.7	–2.37
2472	33	2.7	–2.93
2474	34	2.7	–2.72
2476	35	2.7	–2.3
2478	36	2.7	–2.3
2480	39	2.7	–2.43

Figure 4-22 and Figure 4-23 show the difference in the uncompensated and compensated error.

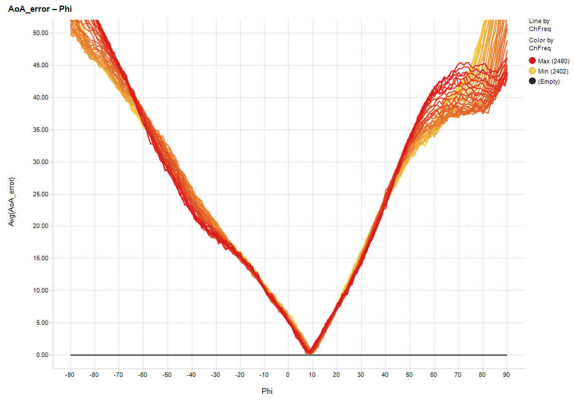

Figure 4-22. PCB + RF Absorbing Material + Tin-Plated Copper Foil + Metal Uncompensated AoA Error

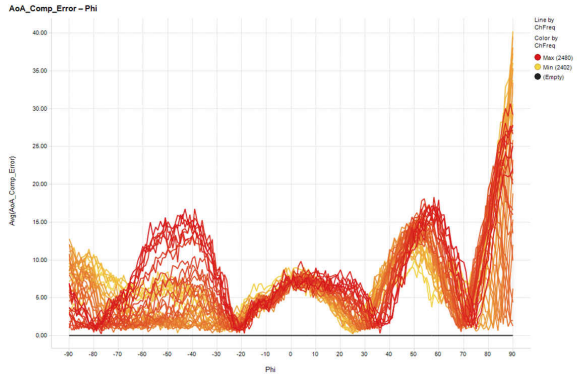

Figure 4-23. PCB + RF Absorbing Material + Tin-Plated Copper Foil + Metal Compensated AoA Error

The error is greatly improved with compensation. Depending on the frequency, this hardware setup shows less than 10° of error from –90° to 40° and 70° to 90°. There is considerable error from 40° to 65° for most frequencies. Better compensation methods could greatly improve this error while still maintaining the full range of ±90°. Figure 4-24 and Figure 4-25 show the uncompensated AoA vs compensated AoA.

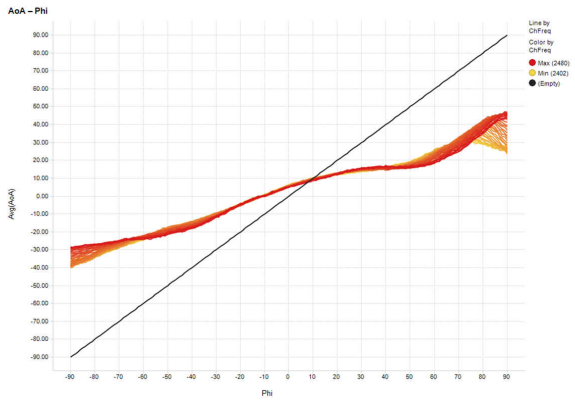

Figure 4-24. PCB + RF Absorbing Material + Tin-Plated Copper Foil Uncompensated AoA Results Over all Bluetooth Low Energy Channels

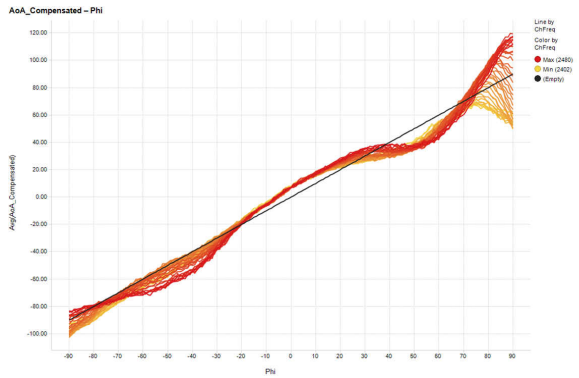

Figure 4-25. PCB + RF Absorbing Material + Tin-Plated Copper Foil + Metal Compensated AoA Results Over all Bluetooth Low Energy Channels

4.2.4 Hardware Setup Compensated Results Comparison

After implementing some basic linear compensation to the three hardware setups with the most linear IQ difference and AoA results, the compensated AoA results can be compared. Figure 4-26 shows all compensated AoA error vs Phi (the actual angle) with the bare PCB at the top, PCB + RF absorbing material + tin-plated copper foil in the middle, and PCB + RF absorbing material + tin-plated copper foil + metal at the bottom.

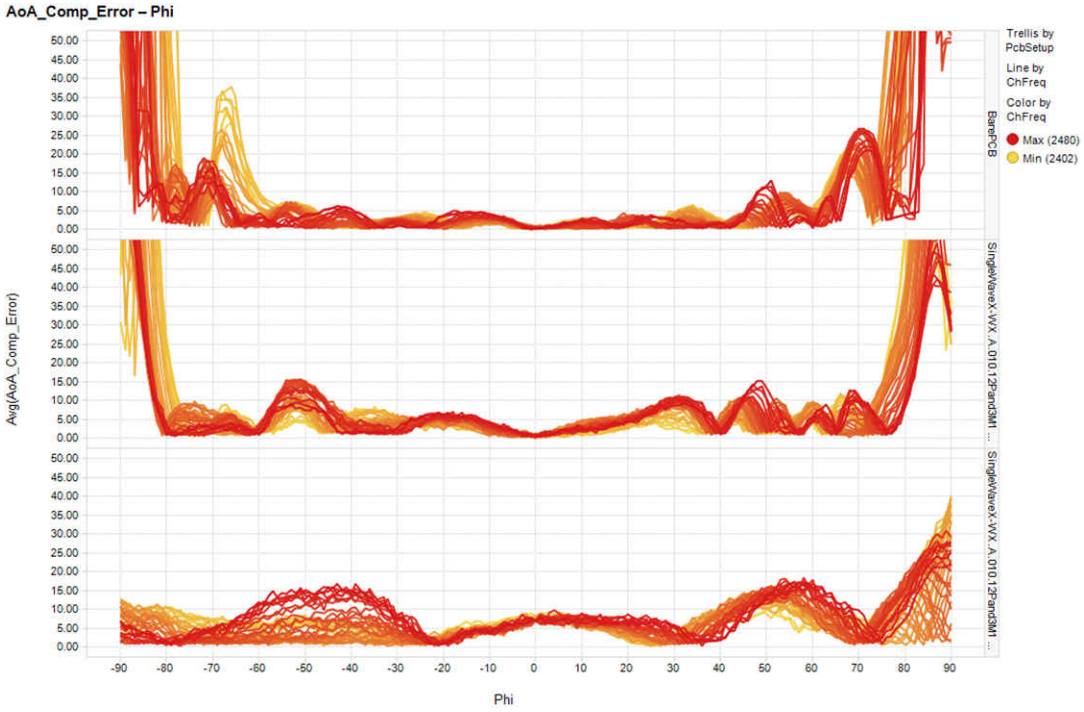

Figure 4-26. Hardware Setup Comparison: Compensated AoA Error vs Phi

The comparison shows that the bare PCB shows the best results from approximately –65° to 65° but is the least accurate outside of that range. Adding the RF absorbing material and tin-plated copper foil reduces the error at the wider angles but at the cost of increased error from –30° to 35°. Adding the metal further decreases the error at the widest angles but also further increased the error from –20° to 20° and 40° to 70°. Again, better compensation could potentially improve the results for all hardware setups. Figure 4-27 shows the comparison of the three hardware setups compensated AoA over Phi in the same order as Figure 4-26.

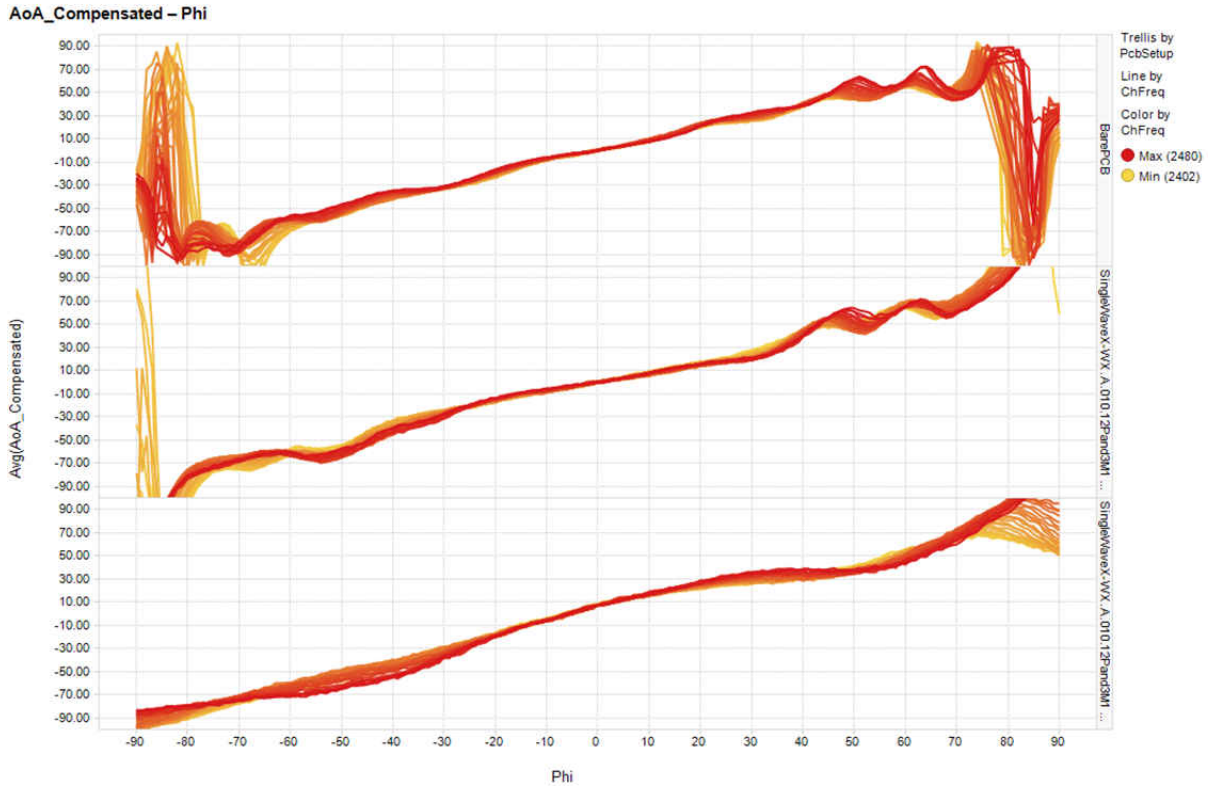

Figure 4-27. Hardware Setup Comparison: Compensated AoA Results

Figure 4-27 shows that for the full ±90° range, the PCB + RF absorbing material + tin-platted copper foil + metal provides the most stable results across all frequencies. All hardware setups become less linear as the angle gets wider, whether positive or negative. In addition, different frequencies provide more accurate results for specific angle ranges. It is important to remember that the antenna efficiency degrades when metal is close by. However, the data shows that the AoA range increases with the metal stand and tin-platted copper foil.

The tests results demonstrate the importance of testing and understanding the performance of the hardware setup. It is recommended to understand the behavior of the IQ difference measurements for a specific hardware setup to improve the AoA calculation and therefore the overall solutions AoA accuracy.

5 References

1. *Bluetooth Core Specification v5.1*
2. Texas Instruments, *TIDA-01632 Bluetooth Low Energy Satellite Module Reference Design*
3. Texas Instruments, *SimpleLink™ Angle of Arrival BoosterPack*
4. Texas Instruments, SimpleLink CC2640R2 SDK
5. Texas Instruments, CC2640R2F-Q1

6 Revision History

Changes from Revision * (July 2019) to Revision A (June 2023)	Page
• Updated the numbering format for tables, figures, and cross-references throughout the document	1

IMPORTANT NOTICE AND DISCLAIMER

TI PROVIDES TECHNICAL AND RELIABILITY DATA (INCLUDING DATA SHEETS), DESIGN RESOURCES (INCLUDING REFERENCE DESIGNS), APPLICATION OR OTHER DESIGN ADVICE, WEB TOOLS, SAFETY INFORMATION, AND OTHER RESOURCES “AS IS” AND WITH ALL FAULTS, AND DISCLAIMS ALL WARRANTIES, EXPRESS AND IMPLIED, INCLUDING WITHOUT LIMITATION ANY IMPLIED WARRANTIES OF MERCHANTABILITY, FITNESS FOR A PARTICULAR PURPOSE OR NON-INFRINGEMENT OF THIRD PARTY INTELLECTUAL PROPERTY RIGHTS.

These resources are intended for skilled developers designing with TI products. You are solely responsible for (1) selecting the appropriate TI products for your application, (2) designing, validating and testing your application, and (3) ensuring your application meets applicable standards, and any other safety, security, regulatory or other requirements.

These resources are subject to change without notice. TI grants you permission to use these resources only for development of an application that uses the TI products described in the resource. Other reproduction and display of these resources is prohibited. No license is granted to any other TI intellectual property right or to any third party intellectual property right. TI disclaims responsibility for, and you will fully indemnify TI and its representatives against, any claims, damages, costs, losses, and liabilities arising out of your use of these resources.

TI’s products are provided subject to TI’s Terms of Sale or other applicable terms available either on ti.com or provided in conjunction with such TI products. TI’s provision of these resources does not expand or otherwise alter TI’s applicable warranties or warranty disclaimers for TI products.

TI objects to and rejects any additional or different terms you may have proposed.

Mailing Address: Texas Instruments, Post Office Box 655303, Dallas, Texas 75265